ELSEVIER

Marine Geology 190 (2002) 493–529

MARINE GEOLOGY
INTERNATIONAL JOURNAL OF MARINE GEOLOGY, GEOCHEMISTRY AND GEOPHYSICS

www.elsevier.com/locate/margeo

Tectonic evolution of the Marmara Sea and its surroundings

Cenk Yaltırak [a,b,*]

[a] *Istanbul Technical University, Faculty of Mines, 80626 Maslak, Istanbul, Turkey*
[b] *Istanbul Technical University, Institute of Eurasian Earth Sciences, 80626 Maslak, Istanbul, Turkey*

Received 1 May 2001; accepted 19 February 2002

Abstract

The basins in the Marmara Sea are the products of a superimposed evolutionary history defined by two different-aged fault systems: the early Miocene–early Pliocene Thrace–Eskişehir Fault Zone and its branches, and the late Pliocene–Recent North Anatolian Fault and its branches. The Thrace–Eskişehir fault and its westward branching secondary fault systems define the early neotectonic signature in the region. The late neotectonic period started at the end of the early Pliocene when the North Anatolian Fault divided the Thrace–Eskişehir fault into four parts. During the late neotectonic period, the North Anatolian Fault extended westward as a number of splays by joining with the Ganos, Bandırma–Behramkale and Manyas–Edremit Fault Zones. The branches of the North Anatolian Fault Zone (NAFZ) caused the evolution of a number of basins, which differ in character depending on the trend and past characteristics of the older branches that became connected. Since the northern branch of the North Anatolian Fault is connected to the N80°E-trending Ganos Fault Zone (GFZ) in the west, a single buried fault has developed in the Marmara Sea, causing the well-known troughs and ridges, superimposed onto the negative flower structure formed by the GFZ in the early neotectonic period. The middle strand, which extends from Iznik Lake to Bandırma, is oriented east–west up to the N60°E-trending Bandırma–Behramkale Fault Zone, then turns southward in the vicinity of Bandırma, forming a region dominated by compressional tectonics. This bending caused N30°E-trending tension in addition to the strike-slip motion between the eastern part of Gemlik Bay and Bandırma Bay. The southern branch of the NAFZ, on the other hand, produced three pull-apart basins with different characteristics along the Yenişehir, Bursa and Manyas segments. The southern branch of the NAFZ connected to the Manyas–Edremit Fault Zone, which is oriented N45°E to the south of Manyas, and the associated bending and rotation caused a N15°E-trending extension in addition to the strike-slip regime between Manyas and Uluabat. The branches of North Anatolian Fault cut through the Thrace–Eskişehir fault at three places: the East Marmara Sea region, in Gemlik Bay, and to the east of Bursa, giving lateral offsets of 58–59, 7–8 and 10–11 km, respectively. The cumulative motion is 75–78 km, corresponding to the total lateral offset of the North Anatolian Fault in the region. The correlation of these offsets with Global Positioning System slip vectors and with stratigraphic results implies that the North Anatolian Fault reached into the Marmara Sea region about 3.5 million yr ago. Tectonic processes forming the Marmara Sea and its environs were initiated by the Thrace–Eskişehir fault and its splays have been most recently controlled by the North Anatolian Fault and its splays during the last 3.5 million yr.

Keywords: Marmara Sea; North Anatolian Fault; Thrace–Eskişehir fault; superimposed tectonics; sub-basin; neotectonics

* Fax: +90-0-212-2856210.
E-mail address: yaltirak@itu.edu.tr (C. Yaltırak).

0025-3227/02/$ – see front matter © 2002 Elsevier Science B.V. All rights reserved.
PII: S0025-3227(02)00360-2

1. Introduction

The 1500-km-long North Anatolian Fault Zone (NAFZ) bifurcates into three branches to the east of the Marmara Sea (Fig. 1A). These branches terminate where the westward escape of the Anatolian Block turns into anticlockwise rotational opening in the northern Aegean Sea and Edremit Bay (Fig. 1B). These three branches demonstrate different kinematic and seismic appearances in the Marmara region. First, the NAFZ bifurcates west of ~30.5°E latitude into two branches (Fig. 1). The northern strand of the North Anatolian Fault (NAFNS) extends from Bolu to Izmit (Şengör, 1979; Bozkurt, 2001), while the second branch extends southward from Bolu and bifurcates once more in the Pamukova Plain at ~30°E latitude (Koçyiğit, 1988) (Fig. 1B). The northern of these latter branches is the middle strand of the North Anatolian Fault (NAFMS), which extends almost east–west along Iznik Lake, Gemlik Bay and Bandırma Bay. It changes direction around the western part of Bandırma Bay and turns southwestward into a fault zone formed of many faults (Fig. 1B). The southern branch of the North Anatolian Fault (NAFSS) is a northeast–southwest-trending fault extending from Pamukova. The NAFSS creates the Yenişehir pull-apart basin together with another fault to the north (Fig. 1B). It extends from Bursa to Manyas, bending southwest from the southern part of the Uluabat Lake, then extends in a WNW–ESE direction until the southern part of Manyas Lake (Fig. 1B). To the southwest of Manyas Lake, the fault changes its direction to S45°W, then extends from Manyas to Edremit, turning into a set of discontinuous short fault segments.

There are different views concerning the position and character of the NAFZ both on land and at sea. The most important debates revolve around the Marmara Sea problem (Crampin and Evans, 1986; Barka and Kadinky-Cade, 1988; Ergün and Özel, 1995; Wong et al., 1995; Okay et al., 1999, 2000; Parke et al., 1999; Le Pichon et al., 1999; Aksu et al., 2000; Siyako et al., 2000; Imren et al., 2001). These recent studies can be classified into three groups: (1) pull-apart and combined models (Barka and Kadinky-Cade, 1988; Wong et al., 1995; Ergün and Özel, 1995; Barka, 1992); (2) models incorporating *en echelon* fault segments (Parke et al., 1999; Siyako et al., 2000; Okay et al., 2000); and (3) models with a single master fault beneath the Marmara Sea (Fig. 2; Le Pichon et al., 1999; Aksu et al., 2000; Imren et al., 2001). The most distinctive structure in the Marmara Sea is a series of east–west-trending troughs separated by NNE–SSW-trending ridges. Here, these are called the West Marmara Trough (WMT; the Tekirdağ Trough of Okay et al., 1999), Middle Marmara Trough (MMT), and East Marmara Trough (EMT; Çınarcık Trough of Okay et al., 2000) (Fig. 3).

Although the initial models for the evolution of the Marmara Sea date from the 1930s, the first modern study concerning seafloor topography and seismic sections is the pull-apart model of Barka and Kadinky-Cade (1988). Subsequently, on the basis of 1670 line-km of shallow seismic reflection data collected in 1987, this pull-apart model was modified to include compressional and tensional rhombohedral blocks to explain the three deep basins ('troughs') in the Marmara Sea (Ergün and Özel, 1995; Wong et al., 1995). During the same period, based on shallow and conventional seismic data gathered on the southern shelf, Smith et al. (1995) identified east–west-trending normal faults and proposed that the southern part of the Marmara Basin was a half-graben. About 1500 line-km of conventional seismic data were collected by R/V *Sismik-1* of the Mineral Research and Exploration Institute of Turkey (MTA)in 1997. Three different working groups interpreted these data, reaching different conclusions. Okay et al. (1999) proposed that a so-called master fault, which borders the southern part of the western Marmara Sea and then arrives on land, is a northeast–southwest thrust fault to the east of the WMT. They also proposed a normal fault in the middle of the trough and a north-thrusting dextral fault to the west of the trough nearest land. Okay et al. (1999) proposed that Ganos Mountain, 10 km wide, 30 km long, and 900 m high in 28-km-thick crust (Aygül and Genç, 1999), formed because of elastic bending associated with this thrust fault geometry. Parke et al. (1999), who interpreted all of the data collected

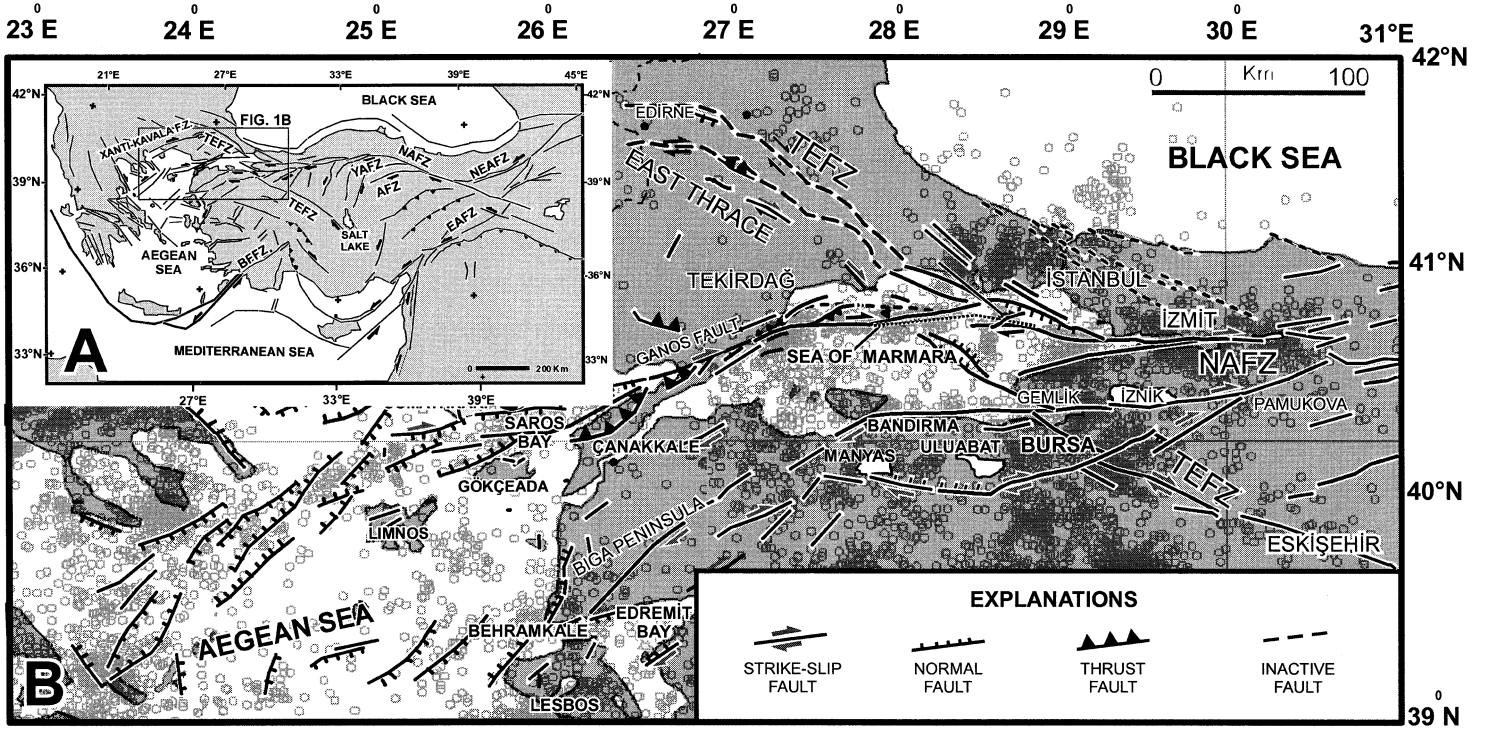

Fig. 1. (A) Simplified tectonic map of eastern Mediterranean region (adapted from Yaltırak et al., 1998). (B) Seismotectonic map of the Marmara Sea region (compiled from Sakınç et al., 1999; Yaltırak, 2000b; Yaltırak et al., 1998). Abbreviations: GFZ, Ganos Fault Zone; TEFZ, Thrace–Eskişehir Fault Zone; BFFZ, Burdur–Fethiye Fault Zone; NAFZ, North Anatolian Fault Zone; EFZ, East Anatolian Fault Zone; NEAFZ, Northeast Anatolian Fault Zone; AFZ, Almus Fault Zone; YEFZ, Yağmurlu–Ezinepazarı Fault Zone. (Compiled from Barka, 1992; Yaltırak et al., 1998; Bozkurt, 2001.)

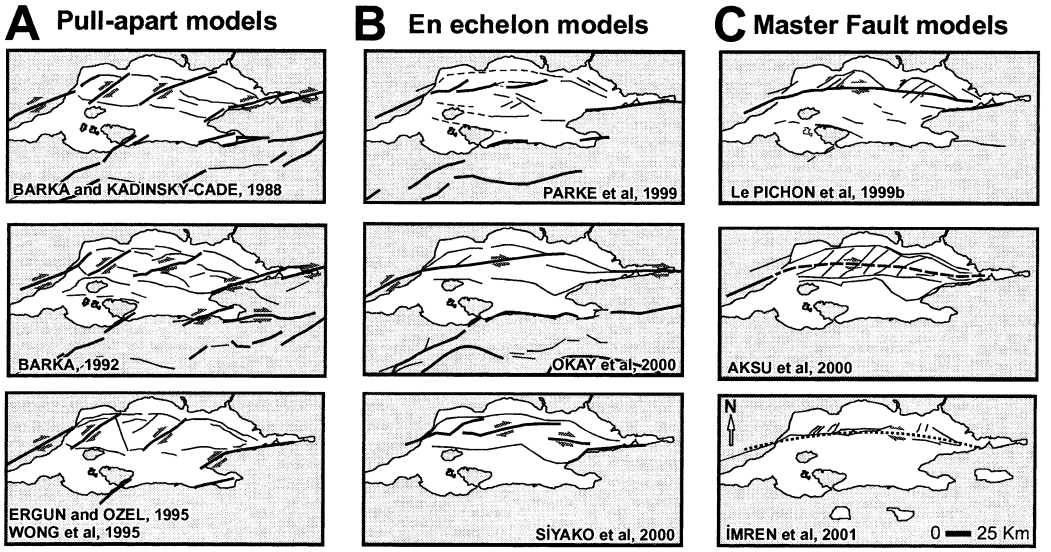

Fig. 2. Tectonic models of the Marmara Sea. (A) Pull-apart models. (B) 'En echelon' models. (C) Master fault models. Bold lines represent the main faults which played active roles in forming the Marmara Sea. The thinner lines show secondary faults.

during MTA's 1997 cruise, suggested that the NAFZ system diminishes in importance in the Marmara region and east–west-trending normal faults caused the evolution of the Marmara Sea. Finally, Le Pichon et al. (1999), who interpreted the same data after the 1999 eastern Marmara earthquakes, claimed that there is a buried master fault extending through the Marmara Sea. These authors named this master fault the Great Marmara Fault and proposed that this main structure passes through the southern boundary of the EMT, along the central axis of the MMT, and along the southern boundary of the WMT (Fig. 3), causing the evolution of the troughs and ridges due to dextral shearing forces. After the 1999 eastern Marmara earthquake, Okay et al. (2000) combined the data sets collected by the MTA on the East Marmara Ridge (EMR) and its western part (314 line-km), with the previous 1997 data set (429 line-km). They proposed that the single master fault model might not be valid, since the fault bifurcates. The master fault functions as a normal fault by bounding the northern edge of the EMT in the Eastern Marmara Sea (Okay et al., 2000), then crosses through the northern part of the eastern ridge and continues N80°W as a strike-slip fault (Okay et al., 2000, figure 2, p. 191). In another article, published after the 1999 earthquakes, Aksu et al. (2000) studied the Marmara fault systems based on 3390 line-km of single-channel shallow seismic reflection data collected by R/V *Piri Reis* in 1995. Aksu et al. (2000) suggested that the Marmara Sea evolved as a negative flower structure, bounded by two west-trending sidewall faults that are linked to a single near-vertical master fault. Siyako et al. (2000) used 5500 line-km of conventional multichannel seismic data collected by the Turkish Petroleum Cooperation to propose that three *en echelon* strike-slip fault segments cross the Marmara troughs forming a negative flower structure, and that the Marmara troughs are bounded by shallowly dipping normal faults. Recently, on the basis of seismic data collected during the MTA 1997 and 2000 cruises (2200 line-km), Imren et al. (2001) modified the model proposed by Le Pichon et al. (1999).

Recent publications employ 8500 line-km of deep seismic data and 5000 line-km of shallow seismic data covering an area 200 km by 80 km in the Marmara Sea (Barka and Kadinky-Cade, 1988; Ergün and Özel, 1995; Wong et al., 1995; Okay et al., 1999, 2000; Parke et al., 1999; Le Pichon et al., 1999; Aksu et al., 2000; Siyako et al., 2000; Imren et al., 2001). Although these studies propose internally consistent interpreta-

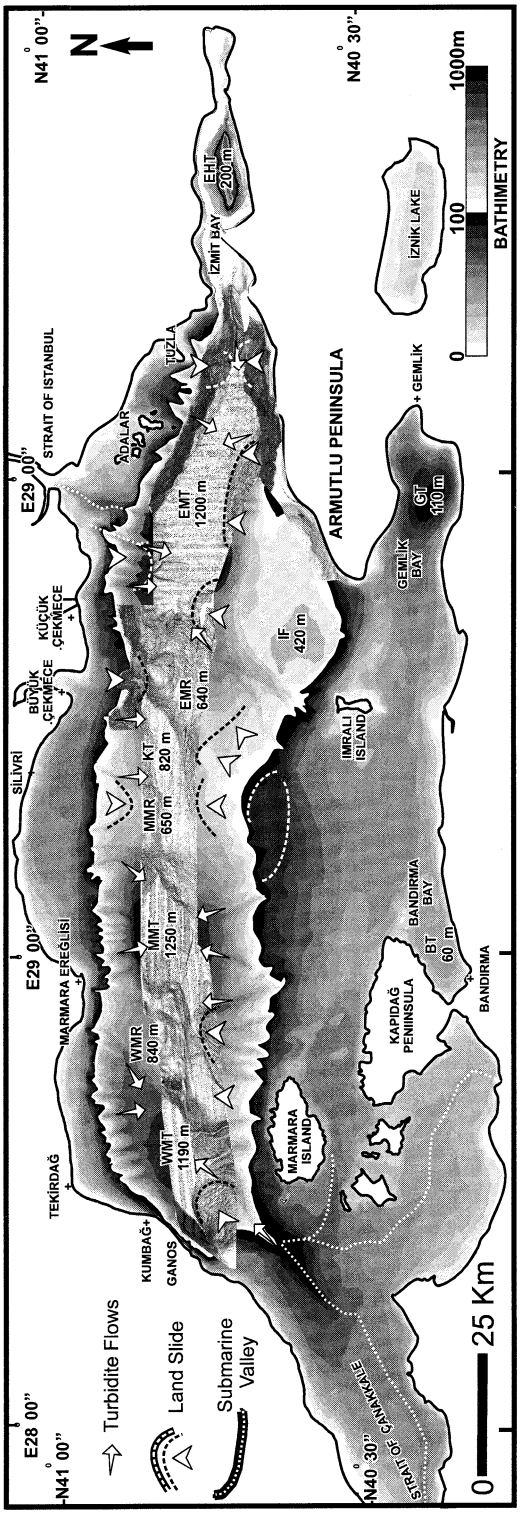

tions, none of them forms a synthesis combining studies on land geology, land tectonics, gravity, magnetics, topography and bathymetry, Global Positioning System (GPS), stratigraphy, basin characteristics, and seismotectonics. In this paper, the full set of available data will be considered, not only for the Marmara Sea but also its environs; all of the geological and geophysical data used in previous works will be reviewed and interpreted in the light of detailed land observations. Using all these of data, the evolution of the faults and basins will be discussed.

2. Data and methods

Two data sets are utilised in this study. The first includes structural and geological maps which were produced from detailed geologic surveys on land. Geological mapping was initiated in 1995 in Eastern Thrace and the Gelibolu Peninsula. Faults were observed from satellite images (Yaltırak, 1996), defined by land seismicity (Perinçek, 1991), and mapped precisely based on field observations (Sakınç et al., 1999). In the southern Marmara region, the disposition of the Thrace–Eskişehir fault (Sakınç et al., 1999) was determined using satellite images and digital topographic maps prepared from SAR interferometry, and was then plotted on the geological maps based on the control of field observations (Yaltırak, 2000a). The gravity and magnetic maps of (Akdoğan, 2000) and digital topography maps were consulted to corroborate fault placement. The depositional units defined during the field observations

Fig. 3. Seafloor morphology and superimposed multibeam image of the Marmara Sea. (Compiled from Ardel and Kurter, 1973; Yılmaz, 1996; Güneysu, 1998; Güneysu, 1999; Aksu et al., 1999; Multibeam image from Turkish Navy, Department of Navigation, Hydrography and Oceanography.) Arrows show landslides and turbidity–current flow directions. Dashed lines (black/white) show landslide boundaries. Abbreviations: WMT, Western Marmara Trough; WMR, Western Marmara Ridge; MMT, Middle Marmara Trough; MMR, Middle Marmara Ridge; KT, Kumburgaz Trough; EMR, Eastern Marmara Ridge; EMT, Eastern Marmara Trough; IF, Imarlı Flat; EHT, Eastern Hersek Trough; GT, Gemlik Trough; BT, Bandırma Trough.

at different localities were compared in a stratigraphic manner. The formations were dated and the depositional environments compared (Yaltırak et al., 1998; Sakınç et al., 1999; Yaltırak et al., 2000a).

The second data set consists of marine seismic profiles. Multichannel conventional seismic sections of Okay et al. (1999), Okay et al. (2000), Siyako et al. (2000), and Imren et al. (2001), and shallow seismic sections of Ergün and Özel (1995), Wong et al. (1995), Smith et al. (1995), and Aksu et al. (2000) were combined and re-interpreted. This re-interpretation has resulted in a new structural map. A bathymetric map was also drawn for this study. The navigation charts of the Turkish Navy and the Department of Navigation, Hydrography and Oceanography were used with 5-m accuracy for shelf areas (Ardel and Kurter, 1973; Yılmaz, 1996; Güneysu, 1998, 1999). For deeper areas below 100-m water depth, bathymetric contours with 50-m depth contours of Aksu et al. (1999) were utilised. These data were combined with the multibeam swath data (20-m grid size) collected by the Department of Navigation, Hydrography and Oceanography along the troughs of the Marmara Sea (Fig. 3). On this bathymetric map, the deep Marmara troughs, which are known since Andrussov (1890), are clearly defined.

The faults traced on the seismic sections were plotted and a simplified structural map was composed for the main faults at sea. From the combination of marine and land data, the fault-bounded structural blocks in the Marmara Sea were defined. The characteristics of these boundary faults are known from fault plane solutions. Finally, palinspastic tectonical evolution maps were drawn for every 500 000 yr using the stratigraphic age determinations in the marine and land areas, GPS slip vectors, and kinematic features of the fault planes.

3. Seafloor morphology of the Marmara Sea

3.1. Shelf areas

The shelf areas can be classified into four regions: Tekirdağ, Silivri, Çekmece, and Adalar. Many canyons cut the shelf edge and continental slopes (Fig. 3). The shelf in the Tekirdağ region narrows between Kumbağ and Marmara Ereğlisi. The arc-shaped Silivri region between Marmara Ereğlisi and Büyük Çekmece has the widest shelf area on the northern side of the Marmara Sea. The shelf of the Küçük Çekmece region becomes narrower toward the Strait of Istanbul, where the shelf edge approaches the coast. The Adalar region is separated from the western shelf area by the Marmara canyon of the Strait of Istanbul (Fig. 3).

On the southern shelf, there are two different areas. To the north of the Armutlu Peninsula, the shelf is narrow (<1 km). Between Armutlu Island and Marmara Island, the widest underwater plain of the Marmara Sea is found (Fig. 3). This plain is between the Kapıdağ Peninsula, Imralı Island and Marmara Island, and extends into Gemlik and Bandırma bays. Its slope is 1–2°. The most interesting features are the islands and small troughs on the seafloor (Fig. 3). The second shelf area occurs to the east of the Strait of Çanakkale, where an underwater valley extends from the strait into the WMT. This valley is connected with two others running southwest of the Kapıdağ Peninsula and Marmara Island (Fig. 3).

3.1.1. Shelf troughs

Gemlik Trough: the deepest point of Gemlik Bay is 110 m deep, 50 m below the elevation of the southern shelf (Fig. 3). Bandırma Trough (BT): this is a triangular-shaped trough separated from the 60–70-m-deep shelf area in Bandırma Bay by a 30 m-deep sill. The trough becomes deeper towards the city of Bandırma. To the east of this trough, on the narrow area between the Kapıdağ Peninsula and Bandırma, a rocky shoal extends between the western part of the shelf and the BT (Fig. 3). East Hersek Trough (EHT): this trough is situated in Izmit Bay. It is a rather narrow trough and its deepest part exceeds 200 m. It is separated from the Marmara Sea by a ridge formed by the sediments of Hersek Delta. The slope of its southern margin is 15°, while gradients are 8–10° along the northern slope (Fig. 3).

3.1.2. Underwater valleys

Çanakkale underwater valley: this is the eastward elongation of the strait. It is more than 50 km in length and terminates at the WMT. Another valley, coming from the western part of the Biga Peninsula, is connected to this valley (Fig. 3). These valleys are shallow, open, 'V-shaped' features connected with other minor valleys. They link to master valley branches on land.

Istanbul underwater canyon: this feature is the north–south-trending extension of the combined system of the Strait of Istanbul and Golden Horn into the EMT. It is a 7-km-long valley deepening towards the trough. There is a dextral strike-slip offset of ~1–2 km between the landward end of this canyon and its southern end (Fig. 3).

3.2. Troughs, slopes and ridges

3.2.1. West Marmara Trough

The WMT is a rhombohedral feature with its long axis trending northeast–southwest (Fig. 3). Its maximum depth is 1190 m, with an average of 1100 m. To the north, along an arc-shaped area, there are canyons and gullies perpendicular to the shore that cut across the continental slope from the 100-m contour down to 1100 m depth as slopes change from 18 to 30° (Fig. 3). To the northwest of the WMT, a wide underwater debris fan progrades to the south. This feature is 10 km long and 8 km wide (Fig. 3). To the south of the WMT, the gradient of the continental slope is 14–24°. Two canyons off Marmara Island extend to the southwest of this trough. There are two more prominent canyons: one is the eastward extension of the Strait of Çanakkale and the other one coincides with the Ganos Fault Zone (GFZ) (Fig. 3). Between these, southeast of the town of Ganos, there is another underwater landslide fan (12×8 km size) that extends from 100 m water depth down to the bottom of the trough (Fig. 3). The surface of this fan, with a slope of about 10°, has a step-like morphology. Bathymetric and swath data suggest that this fan was caused by underwater failures.

3.2.2. West Marmara Ridge

The WMR is located to the east of the WMT. It is 440 m deep and bounded by 840-m-deep valleys at its two sides (Fig. 3). The valley to the north is the boundary between the WMR and the 100-m-deep shelf (Fig. 3). To the south, a fault step in front of Marmara Island, which belongs to the NAFZ, forms the southern boundary of the WMR. There is a valley here between the shelf and the WMR that almost coincides with the NAFNS and extends to the MMT.

3.2.3. Middle Marmara Trough

The MMT contains the deepest point (~1250 m) in the Marmara Sea (Fig. 3). Many canyons perpendicular to the shelf edge enter the MMT from the northern continental shelf. These canyons terminate near the edge of the basin floor at ~1200 m depth. To the south, canyons starting near the shelf edge extend in a NNW–SSE direction towards the western side of the MMT (Fig. 3). In the south–central part of the MMT, an underwater fan with a gentle slope covers a large area.

3.2.4. Middle Marmara Ridge

The Middle Marmara Ridge (MMR) is situated to the east of the MMT (Fig. 3). The MMR is uplifted above the troughs to the east and west. An east–west-trending valley cuts through its central part, so that the centre of the ridge is its deepest part (~650 m). Convex bulges in the slopes north and south of the central basinal area form the ends of the MMR (Fig. 3).

3.2.5. Kumburgaz Trough

The Kumburgaz Trough (KT) is an 820-m-deep trough located to the east of the convex central valley traversing the MMR (Fig. 3). It has the shape of an ellipse extending ENE–WSW and appears to have formed by partial filling of a valley during uplift of the MMR (Fig. 3).

3.2.6. East Marmara Ridge

The EMR is situated to the west of the KT (Fig. 3). It is a 640-m-deep rise trending in an east–west direction for about 24 km, located between the KT and the EMT. There is a 400-m elevation difference between the western and east-

ern edges of the EMR, the west side being shallower. Relative to its height, this is a rather wide ridge (Fig. 3).

3.2.7. East Marmara Trough

The easternmost depression in the Marmara Sea is the triangular-shaped EMT (Fig. 3). The widest part (10 km) of this 1200-m-deep trough is located to the west. The EMT becomes narrower eastward as it approaches the western part of Izmit Bay (Fig. 3). In the Adalar region (Prince Islands), many canyons extend down to the bottom in a north–south direction. In its western part, to the south of the Strait of Istanbul, large underwater fans supplied by slope failures are evident in front of these canyons (Alpar and Yaltırak, 2000). Offshore Tuzla, ridges between the canyons are eroded in the shape of concave-northwards arcs (Fig. 3). To the south of the EMT, there are also many canyons extending downslope from the Armutlu Peninsula (Fig. 3). The convex anomaly, 20 km long and 1 km wide, extending into the trough at ~29°E latitude is an underwater landslide (Alpar and Yaltırak, 2000). Along the southwestern part of the EMT, the slopes are rather smooth. To the west of this smooth slope, two canyons extend from the vicinity of Imralı Island toward the trough (Fig. 3).

3.2.8. Imralı Flat

The Imralı Flat (IF), which is situated in the area between Imralı Island and the southwest edge of the EMT, has a different morphology than either the shelves and the troughs. The deepest point on this plain is at ~−420 m. It becomes shallower (to ~300 m) towards the northeast. The IF has a rhombohedral shape (20×16 km). There are no deep or apparent canyons along the southern slopes (Fig. 3).

4. Regional geology and basins

There are two main sedimentary successions in the Marmara region, with different stratigraphic features. These formed during the early Miocene–early Pliocene and late Pliocene–Recent. These sequences developed during the activation of two different fault systems: the Thrace–Eskişehir Fault Zone (TEFZ), and extensions of the NAFZ (Fig. 1). The Thrace Neogene Basin developed under the control of the GFZ, the Bandırma–Behramkale Fault Zone (BBFZ) and the Manyas–Edremit Fault Zone (MEFZ), the TEFZ itself and its splays. The basins of the Marmara Sea, Saros, Manyas–Ulubat, Bursa, Yenişehir, Iznik and Gönen developed under the control of the Marmara strands of the NAFZ (Fig. 4).

4.1. Thrace Neogene Basin (early Miocene–early Pliocene)

The Thrace Neogene Basin can be divided into three early Miocene–early Pliocene sub-basins, mutually related laterally and covering the modern basins of Southern Marmara, the Marmara Sea and Eastern Thrace (Fig. 4). The northernmost one is the Ergene Sub-basin (ES-B) developed under the control of the TEFZ (Fig. 4). To the south, the Gelibolu–Marmara Sub-basin is located on the GFZ where it was inverted from the TEFZ (see Fig. 4; GMS-B). The other basin is the Southern Marmara Sub-basin, which covers the southern shelf of the Marmara Sea and adjacent land area. It is situated above the BBFZ and the MEFZ that were inverted from the TEFZ (Figs. 4 and 5).

4.1.1. Ergene Sub-basin

The central part of the East Thrace Peninsula is underlain by sediments deposited in the early Miocene–early Pliocene ES-B (Figs. 4 and 5). The ES-B rests unconformably on upper Oligocene lacustrine units at its base and conglomerates toward the basin edges. The fossils found at the base of the basin fill indicate an age of early–middle Miocene (Sakınç et al., 1999). The sequence passes upward into braided river deposits. Andesitic and shoshonitic volcanic rocks are intercalated with these sediments, and intrusive equivalents cut these units locally along the TEFZ. These volcanics give radiometric ages of 21–15 Ma and basic volcanic rocks give 15–5 Ma (Yılmaz and Polat, 1998). In the ES-B, the youngest units are lacustrine limestones and intercalated sandstones deposited in a zone of normal faults

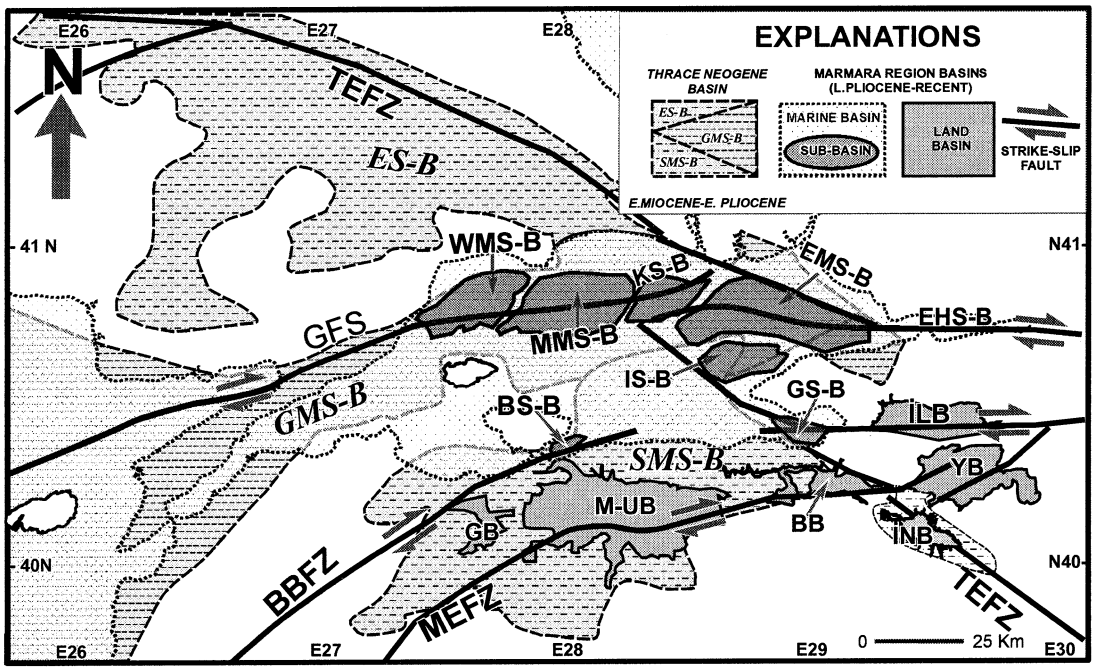

Fig. 4. Early and late neotectonic features superimposed on the basins of the Marmara region. Abbreviations of main fault zones: TEFZ, Thrace–Eskişehir Fault Zone; GFZ, Ganos Fault Zone; BBFZ, Bandırma–Behramkale Fault Zone; MEFZ, Manyas–Edremit Fault Zone. (Compiled from Siyako et al., 1989; Yaltırak et al., 1998, 2000b; Sakınç et al., 1999.) Abbreviations: (1) sub-basins in Thrace Neogene Basin: ES-B, Ergene Sub-basin; GMS-B, Gelibolu–Marmara Sub-basin; SMS-B, South Marmara Sub-basin; (2) Marmara region basins, (a) Marmara Sea basins: WMS-B, West Marmara Sub-basin; MMS-B, Middle Marmara Sub-basin; KS-B, Kumburgaz Sub-basin; EMS-B, East Marmara Sub-basin; BS-B, Bandırma Sub-basin; GS-B, Gemlik Sub-basin; EHS-B, Izmit Sub-basin; (b) Marmara land basins: ILB, Iznik Lake Basin; YB, Yenişehir Basin; INB, Inegöl Basin; BB, Bursa Basin; M-UB, Manyas–Uluabat Basin; GB, Gönen Basin.

that were formed by the southward migration of the TEFZ. Alluvial fans composed of upper Pliocene–Quaternary reddish conglomerates unconformably overlie all these units and also the TEFZ (Fig. 5) (Sakınç et al., 1999).

4.1.2. Gelibolu–Marmara Sub-basin

This sub-basin covers the area of the central and western part of the Marmara Sea, Gulf of Saros and Gelibolu Peninsula (Figs. 4 and 5). Speckled mudstones overlie the basement unconformably, passing upward into braided fluvial deposits and contemporaneous shoreline facies (Sakınç et al., 1999). Fossils indicate an early to early–late Miocene age (Yaltırak et al., 1998; Sakınç et al., 1999). The thickness of the basin fill varies, and becomes thinner towards the fault-controlled basin edges. In the Alçıtepe borehole on the Gelibolu Peninsula, the succession is 1000 m thick (Yaltırak et al., 1998; Yaltırak and Alpar, 2002a). Uppermost, lagoonal, fossiliferous limestone layers (late Miocene–early Pliocene) are intercalated with siliciclastics deposits (Yaltırak et al., 1998; Sakınç et al., 1999). Toward the basin edges, the fluvial series observed at the base pass laterally into more distal central basin deposits. On the Gelibolu Peninsula, upper Pliocene–upper Pleistocene alluvial fan units rest unconformably above this concordant sequence; they accumulated under the influence of the Anafartalar Thrust Fault (Fig. 5) (Yaltırak et al., 2000a). During early Miocene–early Pliocene, the GMS-B was developed over a fault system in which negative and positive flower structures operated together, under the control of the dextral GFZ. The gently dipping normal faults, which bound the shelf edges of the modern western and central Marmara Sea, and ENE–WSW-trending master fault

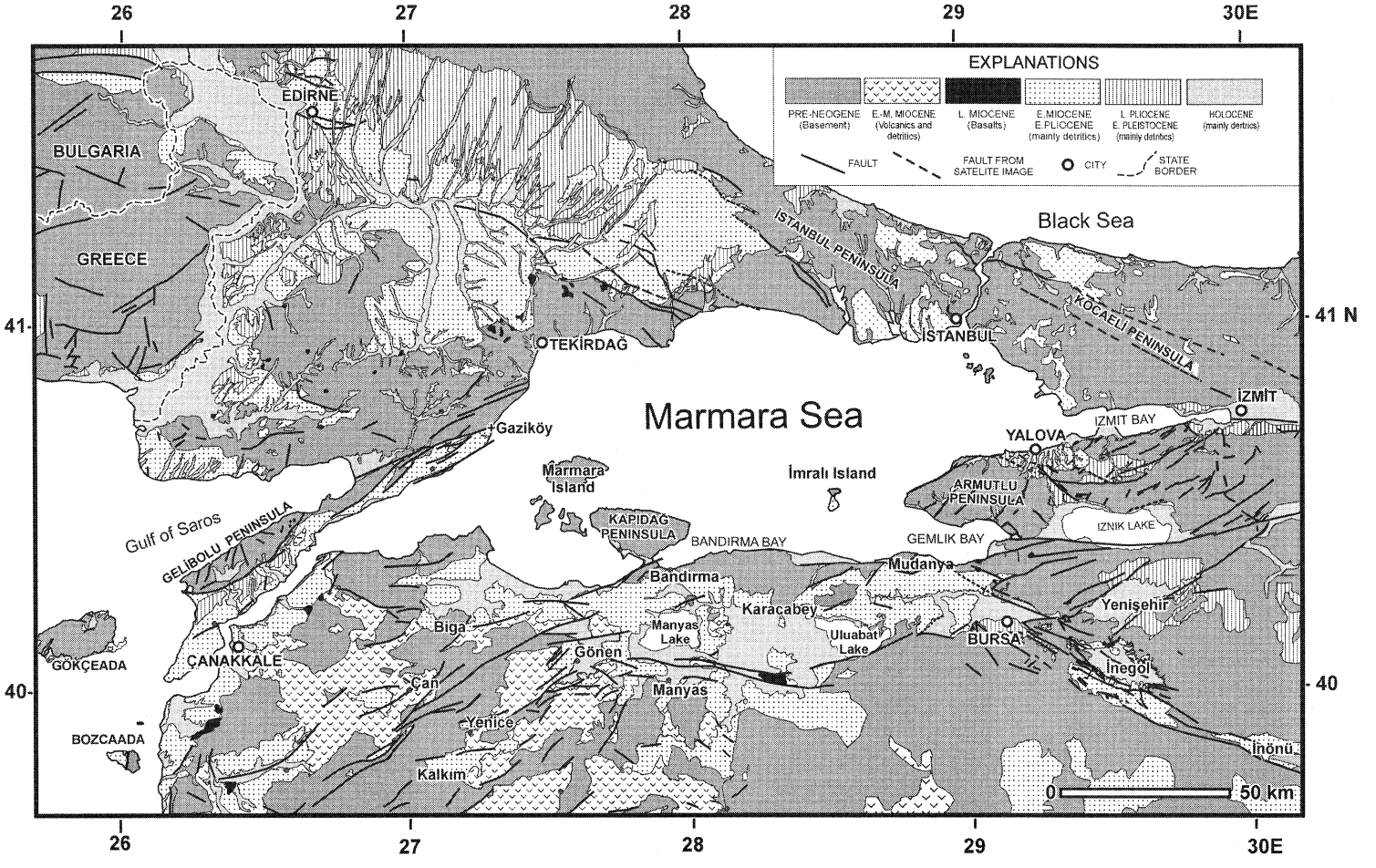

Fig. 5. Geological map of the Marmara region. (Compiled from Ergül et al., 1986; Siyako et al., 1989; Yaltırak et al., 1998; Sakınç et al., 1999; Yaltırak and Alpar, 2002b; Alpar and Yaltırak, 2002 and field study.)

controlled the GMS-B. In the area placed between these faults, the sediments, which become as thick as 1000 m towards Gelibolu, were deposited on the basinal axis.

4.1.3. South Marmara Sub-basin

The Neogene series penetrated by boreholes on the southern Marmara shelf are made up of lacustrine units intercalated with volcanic rocks at the base (Marathon Petroleum, 1976). Upward, these units gradually pass into strata equivalent to the multicoloured terrestrial series observed at the base of the GMS-B (Marathon Petroleum, 1976). These units seem to be the lateral continuation of the area between Gelibolu and Gaziköy on the southern Marmara shelf (Figs. 4 and 5). The South Marmara Sub-basin (SMS-B), which is situated between Gemlik and Bandırma and split into two by the Mudanya–Bandırma uplift under the effect of the NAFZ at present, contains a fill of conglomerates and sandstones around Bursa, Manyas, Uluabat and northward. To the south, the dominant units are sandstones intercalated with volcanic ash and occasional coal layers. The thickness of these units is rather variable (Ergül et al., 1986). The sandstone units are locally folded and overturned, showing local internal unconformities. Their ages cover a period between the middle Miocene and early Pliocene (Ergül et al., 1986; Emre et al., 1998; Yaltırak, 2000a). The faults controlling the SMS-B are those extending westward from the TEFZ, with similar characteristics to those of the GFZ (Figs. 4 and 5). These are the BBFZ to the north and the MEFZ to the south (Figs. 4 and 5).

4.2. Marmara region basins (late Pliocene–Recent)

The Marmara basins are superimposed, under the control of the NAFZ, on the component sub-basins of the Thrace Neogene Basin (Fig. 4). The sediments were deposited in the late Pliocene and later, unconformably above the Thrace Basin (Figs. 4 and 5) (Sakınç et al., 1999). Middle Miocene–lower Pliocene units on the Istanbul, Kocaeli and Armutlu Peninsulas represent low-energy depositional environments (Sakınç et al., 1999; Alpar and Yaltırak, 2002). These units are overlain by small-scale basins reflecting the effects of the NAFZ (Figs. 4 and 5).

4.2.1. Marmara Sea Basin

Sediments in the Marmara Sea Basin (i.e. the modern Marmara Sea) unconformably overlie a variety of older rocks. This depression started its evolution in the late Pliocene, superimposed on units of early Miocene–early Pliocene age belonging to the basins of Marmara–Gelibolu and South Marmara (Fig. 4) (Yaltırak, 1996; Yaltırak et al., 2000a). On the northern shelf, the Neogene units have been completely eroded except in the area around and to the south of Istanbul. The thickness of the Neogene series is about 1000 m in the Doluca and Işıklar boreholes drilled on the south and west Marmara shelves (Marathon Petroleum, 1976; Yaltırak et al., 1998; Yaltırak and Alpar, 2002a). The Marmara Sea Basin can be divided into eight sub-basins that can be defined by troughs and ridges of different depths and sizes (Figs. 4 and 5). Five of them are on the northern strand of the NAFZ. Three of them are different from the rest in terms of their depths and sizes. Twenty-six published multichannel seismic profiles (Okay et al., 1999; Okay et al., 2000; Siyako et al., 2000; Imren et al., 2001), cutting across these sub-basins, were reinterpreted and sixteen of these, together with 3390 line-km of high resolution seismic data (49 lines) have been used in this study (Fig. 6).

The Marmara Sea Basin, which is defined by the present coastline, is made up of deep troughs and bounding shelf areas. These deep troughs each have different basinal characteristics and we denote them as sub-basins in this study, instead of using the term ‘trough’, which is a morphological term. For example, the Imralı Trough (Okay et al., 2000) has no characteristics of a morphological trough. On the contrary, the area northeast of Imralı Island is a step-shaped platform (Fig. 3), 400 m below present sea level. It is located below a shelf in the shape of a isosceles triangle, with two sides of 25 km and a base line of 30 km, to the west of the Armutlu Peninsula. This implies that this platform is not a trough, and should be termed the Imralı Sub-basin due

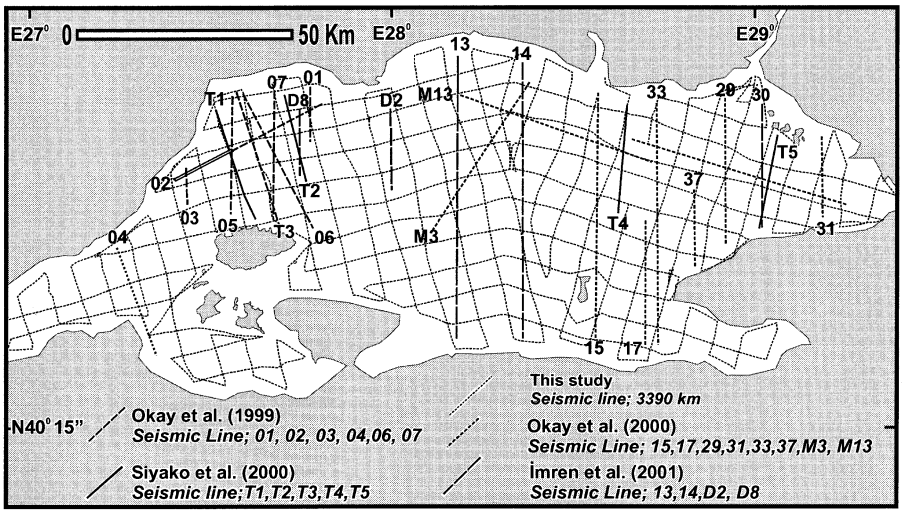

Fig. 6. Seismic Line location map. This study includes two different types of seismic sections. Thin dashed lines are one-second-penetration high-resolution seismic profiles (data from Ali Aksu and Richard Hiscott, Memorial University of Newfoundland; total 3390 km). Multichannel deep-penetration seismic profiles are from Okay et al. (1999, 2000), Siyako et al. (2000), and Imren et al. (2001).

to its depositional characteristics and bounding faults. Similarly, the troughs in the central Marmara Sea must be considered neighbouring sub-basins separated by saddles. Underwater failures, turbidite fans, abyssal plain deposits, deformed ridges and basin-controlling faults serve to define these sub-basins. In conclusion, we prefer using the term 'sub-basin', rather than 'trough', in order to emphasise both the sedimentary units and faults.

4.2.1.1. West Marmara Sub-basin

The maximum depth of this sub-basin is 1190 m. Except along its eastern side (640 m), it is bounded by shelf areas (100 m). This rhomboidal sub-basin covers the area of the WMT and its environs (Figs. 3 and 4). The deposits in the West Marmara Sub-basin (WMS-B) are thicker than 2000 m (Okay et al., 1999). The WMS-B is interpreted as a negative flower structure which formed under the control of the northern strand of the North Anatolian Fault, which passes to the south. The block to the south of this fault contains folded sediments (Fig. 7, Seismic Lines 05 and 06). In this part of the WMS-B, deposits north of the fault are horizontal (Fig. 7, Seismic Lines 05 and 06). Due to the releasing bend nature of the main fault, normal faults can be seen in the seismic profiles. The folding to the south, in contrast, is caused by dextral shearing of the southern block. To the southwest of the sub-basin, imbricated landslides have prograded northward by overlapping horizontal deposits of the basin floor (Figs. 3 and 8, Seismic Line 03). The imbricated geometry of these landslide packages (Fig. 8) has been interpreted as a thrust fault by Okay et al. (1999), who believed that the complex deposits overlying the horizontally bedded sediments were in the hanging wall of the thrust. However, this complex structure corresponds to a typical landslide complex; its lineated surface is evident on the multibeam bathymetry map (Fig. 3).

To the northwest, a low-angle normal fault bounds this sub-basin (Fig. 7, Seismic Line 05). Young deposits overlap this fault. In this area, there are no landslides similar to those observed south. Instead, wide submarine fans spread basinward in front of many small canyons (Fig. 3). To the east of the WMS-B, the WMR has been uplifted under the control of a northeast–southwest-trending thrust fault leading to folding of the eastern part of the fill of the sub-basin (Fig. 7, Seismic Lines 01 and D8). The WMR is completely com-

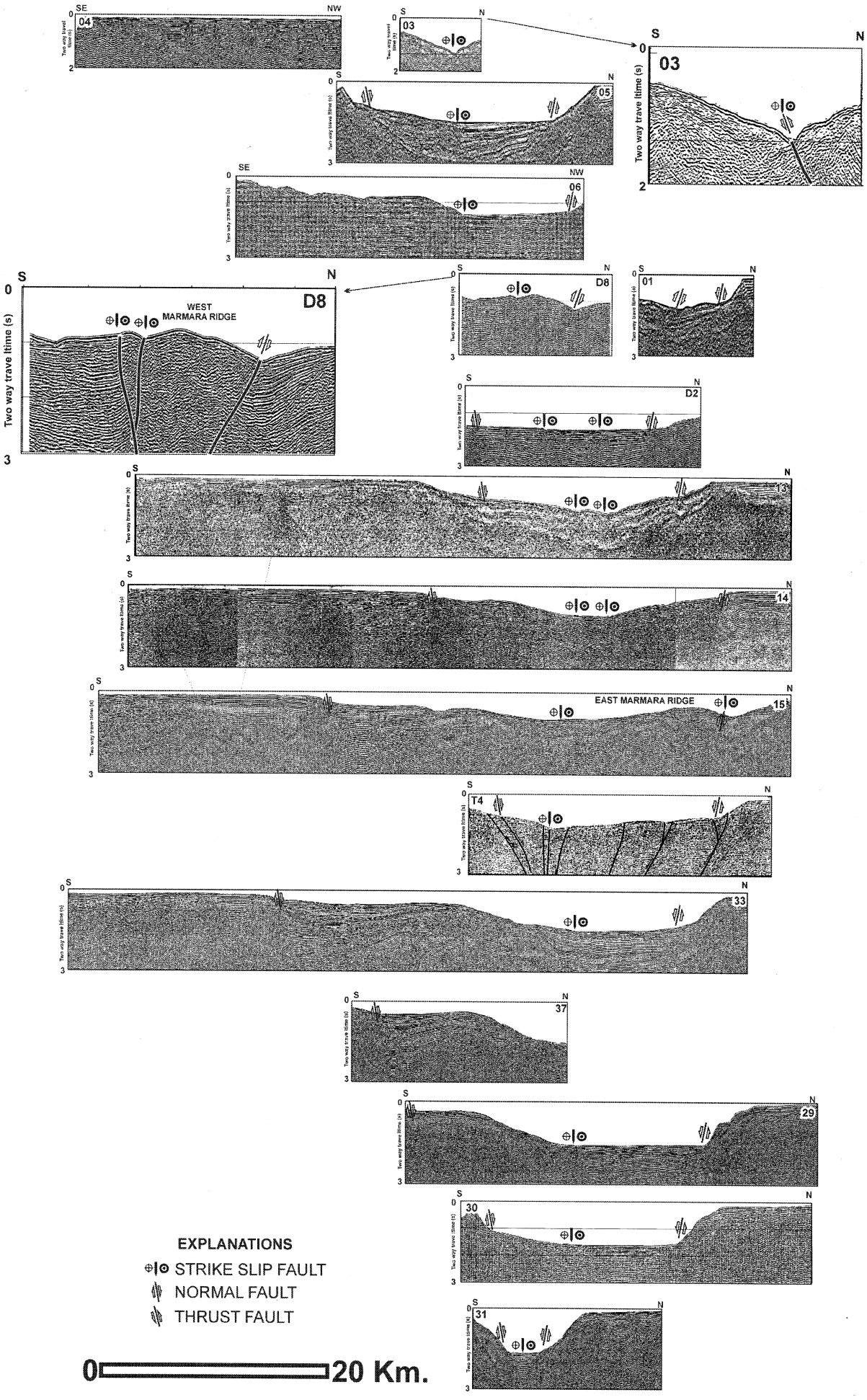

Fig. 7. Re-interpreted and not interpreted time-migrated seismic reflection profiles (from Okay et al., 1999, 2000; Siyako et al., 2000; Imren et al., 2001). Seismic Lines 03 and D8 were re-interpreted in this study. Seismic line T4 was interpreted by Siyako et al. (2000).

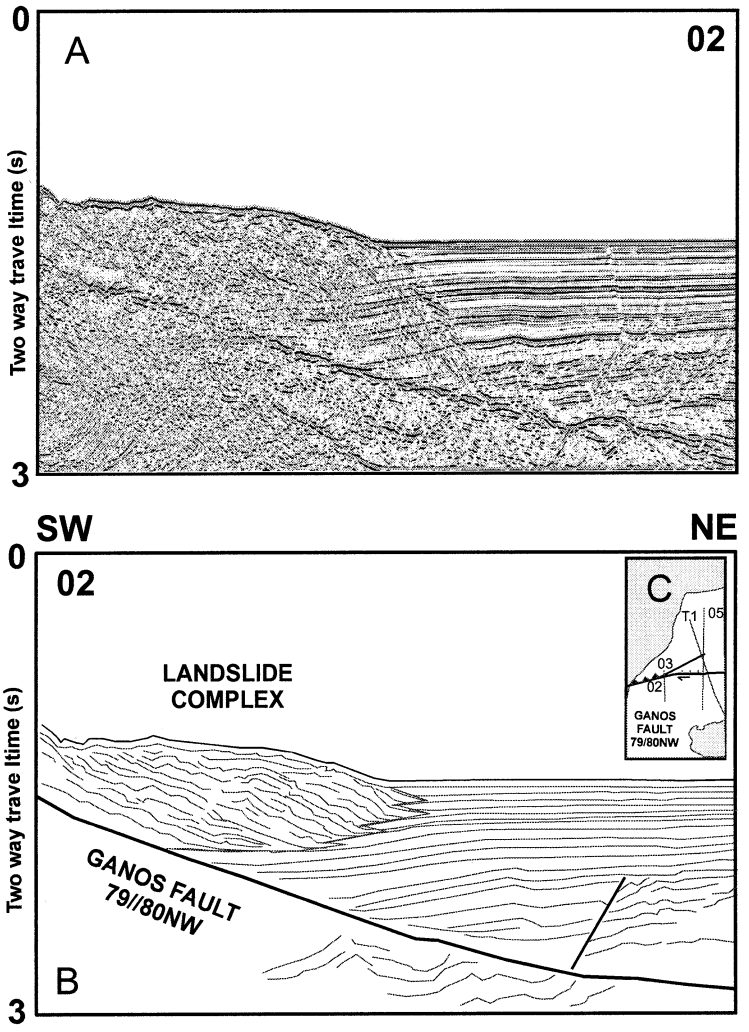

Fig. 8. Not interpreted (from Okay et al., 1999)(A) and re-interpreted (this study) (B) time-migrated seismic reflection profiles along Seismic Line 02. This seismic line shows a landslide complex and the North Anatolian Fault North Segment (Ganos Fault). (C) Location of the seismic line and position of the northern segment of the North Anatolian Fault.

posed of folded sediments and its northern boundary has a thrust character (Fig. 7, Seismic Line D8).

4.2.1.2. Middle Marmara Sub-basin

The Middle Marmara Sub-basin (MMS-B), located in the middle of the Marmara Sea (Fig. 4), resembles a parallelogram. It includes the 1250-m-deep MMT (Fig. 3) and also the gentle surrounding slope areas. northwest–south-east-trending, step-wise normal faults mark the east and west margins of the basin. The other two margins of the basin are the southern and northern shelves landward of gently dipping normal faults (Figs. 6 and 7, Seismic Line D2). The northern strand of the NAFZ crosses the centre of the basin in a direction of N80°E (Figs. 3, 4, 6 and 7, Seismic Line D2). The basin is under the control of the normal faults which developed due to dextral shearing forces. The sediment thickness is more than 2.5 km (Imren et al., 2001), supplied through the canyons extending from the southern and northern shelves (Fig. 3).

4.2.1.3. Kumburgaz Sub-basin

To the northeast of the MMR, the northeast–southwest-elongated Kumburgaz Sub-basin (KS-B) is 800 m deep (Figs. 6 and 7, Seismic Line 14). Along its northern side, the KS-B is controlled by a strike-slip fault, almost vertical but dipping southward and with a normal component of motion. There is also a thrust fault bounding the northwest edge of the EMR (Figs. 3, 4, 6 and 7, Seismic Line 15). Younger sediments are flat lying but older layers become progressively more folded.

4.2.1.4. East Marmara Sub-basin

The East Marmara Sub-basin (EMS-B) has the shape of an acute triangle between the Kocaeli and Armutlu Peninsulas. It includes the eastern flanks of the EMT and EMR (Figs. 3 and 4). The northern edge of this sub-basin is outlined by normal faults, which are almost vertical to the east, while dipping southward to the west (Figs. 6 and 7, Seismic Lines T4, 33, 29, 30). The southern edge of this sub-basin, on the other hand, is outlined by the eastern segment of the northern strand of the NAFZ, which is dextral strike-slip fault trending east–west and dipping northward (Figs. 6 and 7, Seismic Lines 29, 30, 37, 33). To the west of the sub-basin, the mean sea bottom slope is about 8° between a 12-km-wide area forming the deepest part of the basin (1200 m) and the top of the EMR (500 m). Young deposits in the western part of the basin are folded and even imbricated due to dextral shearing; this shearing has also caused the eastern flank of the EMR to be folded and uplifted (Figs. 6, 7 and 9A,B, Seismic Lines 15, M13). The EMR is an anticline formed by compression, but the near-surface faults record shallow gravity-driven extension along the anticline axis and give a wavy appearance to the surface of this ridge (Fig. 9B,C). These structures were interpreted as mega-ripples by Imren et al. (2001) and as folds by Okay et al. (2000). Similar structures elsewhere in the Eastern Mediterranean region were considered as mega-ripples by Ediger et al. (2000). However, these other structures are also clearly shallow normal faults (A.E. Aksu, pers. commun., 2001) like those on the EMR (Fig. 9C).

4.2.1.5. East Hersek Sub-basin

The East Hersek Sub-basin (EHS-B) covers a portion of Izmit Bay east of the Hersek Delta. Its deepest point is 204 m in the EHT (Fig. 3). This sub-basin is developing on the releasing bend of the northern strand of the NAFZ, caused by small jumps between related fault segments where the NAFZ enters the Marmara Sea. In the eastern parts of this rather young sub-basin, the Holocene deposits unconformably overlie acoustic basement (Alpar and Yaltırak, 2002).

4.2.1.6. Imralı Sub-basin

This sub-basin lies below the 300–400 m-deep IF (Fig. 3), located between the EMT and the southern Marmara shelf off the Armutlu Peninsula. The IF becomes shallower northwestward and forms the centre of this sub-basin (Fig. 3). Consistent with the dextral movement of the Imralı Fault Zone (IFZ) and the NAFNS, but also reflecting the normal component of motion on the IFZ, this sub-basin has developed due to tilting of the hanging-wall block (Figs. 3, 4, 6, 7, Seismic Lines 15, 33). Dextral faults extending along the northwest coast of the Armutlu Peninsula accommodate the subsidence of the basin floor (Fig. 7, Seismic Line, and Fig. 10).

4.2.1.7. Bandırma and Gemlik Sub-Basins

The Bandırma Sub-Basin (BS-B) and the Gemlik Sub-basin (GS-B) are situated on the middle strand of the NAFZ near the south coast of the Marmara Sea (Figs. 1 and 10). They are located in Bandırma and Gemlik Bays. The GS-B is situated at a water depth of 110 m and has the shape of an ellipse with a northwest–southeast major axis. It is a pull-apart basin caused by the intersection of the middle strand of the NAFZ with an older northwest–southeast-oriented fault system (Yaltırak and Alpar, 2002b). The BS-B covers an area which is separated from the rest of the Marmara Sea by a 60–70 m-deep sill east of the triangular BT (Fig. 3). It has developed above a small-scale releasing bend where the west-trending

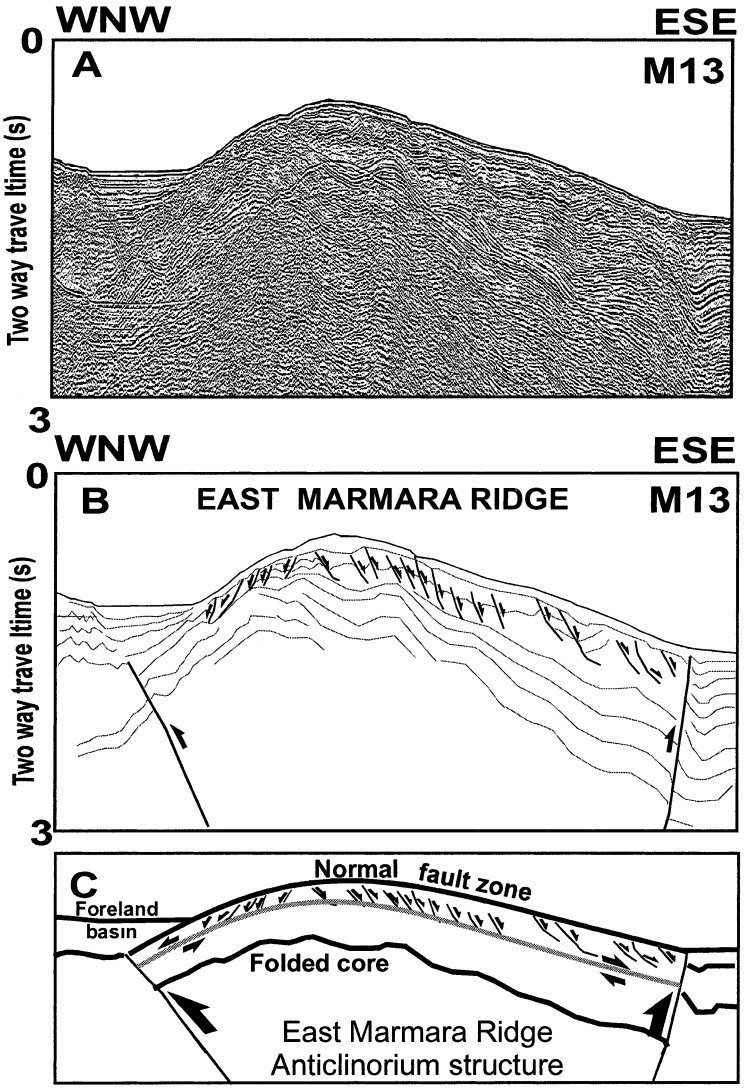

Fig. 9. Not interpreted (from Okay et al., 2000) (A) and re-interpreted (this study) (B) time-migrated seismic reflection profile along Seismic Line M13. (C) This seismic line shows the EMR. The anticlinorium is controlled by two major thrust faults. While folding processes are dominant in the core of the anticlinorium, upward some domino-type shallow normal faults developed on a detachment surface due to the extension occurring on that surface.

middle strand of the NAFZ bends southwest at Bandırma Bay.

4.2.2. Iznik Lake Basin

Iznik Lake Basin (ILB) is located beneath Iznik Lake. It has subsided under the control of the middle strand of the NAFZ, located near its southern shoreline (Fig. 5), and step-wise normal faults to the north, which are oblique to the strike-slip fault (Figs. 3, 4 and 10). It is separated from Gemlik Bay by a narrow valley. Quaternary alluvial fans occur in front of the faults along the southern shores of the lake (Figs. 5 and 10). In this area there are many step-wise and small-scale normal faults, which are parallel to the master fault.

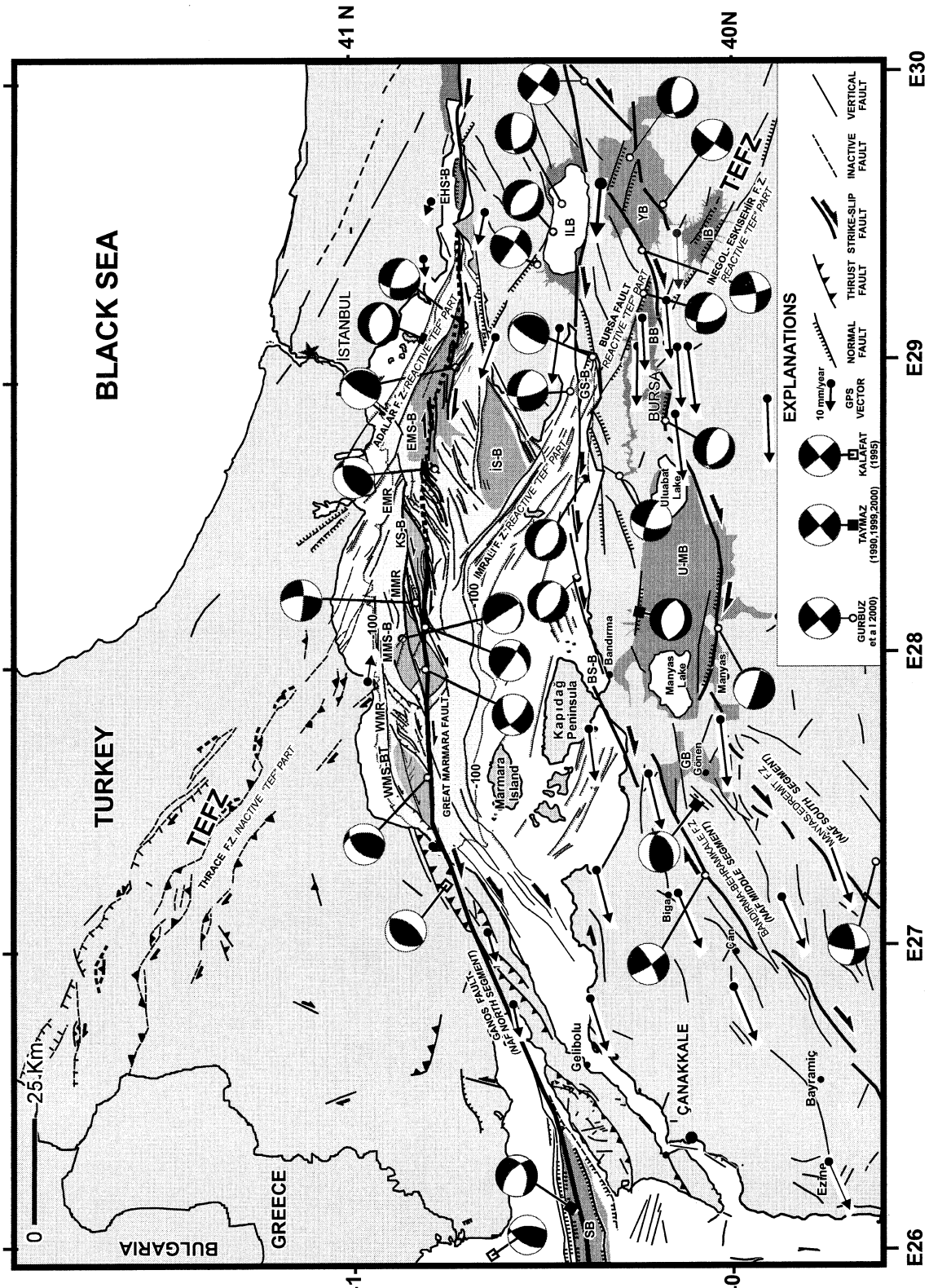
BLACK SEA
TURKEY
GREECE
BULGARIA
ISTANBUL
TEFZ
THRACE F.Z. INACTIVE 'TEF' PART
ADALAR F.Z. REACTIVE 'TEF' PART
İMRALIF Z. REACTIVE 'TEF' PART
BURSA FAULT REACTIVE 'TEF' PART
İNEGOL-ESKİŞEHİR F.Z. REACTIVE 'TEF' PART
GREAT MARMARA FAULT
İSPANOS FAULT (NAF NORTH SEGMENT)
BANDIRMA-BERGAMA FAULT (NAF MIDDLE SEGMENT)
MANYAS SEGMENT (NAF SOUTH SEGMENT)
EMS-B
IS-B
KS-B
GS-B
BS-B
SB
EHS-B
ILB
YB
BB
UMB
GB
WMS-BT
WMR
MMS-B
EMR
MMR
Marmara Island
Kapıdağ Peninsula
Gelibolu
Bandırma
Manyas Lake
Uluabat Lake
BURSA
Gönen
Biga
Gan
ÇANAKKALE
Bayramiç
Ezine
EXPLANATIONS
GURBÜZ et al (2000)
TAYMAZ (1990,1999,2000)
KALAFAT (1995)
GPS VECTOR
10 mm/year
NORMAL FAULT
THRUST FAULT
STRIKE-SLIP FAULT
INACTIVE FAULT
VERTICAL FAULT
25 Km
0
E26
E27
E28
E29
E30
41 N
40N
N41
N40

4.2.3. Yenişehir Basin

The Yenişehir Basin (YB) is located on land atop the southern branch of the NAFZ (Figs. 5 and 10). It is a pull-apart basin developed due to jumping of the southern branch of the NAFZ to another nearby dextral segment. The basin started to develop in the late Pliocene. The rhombohedral Yenişehir Plain forms the centre of this basin (Figs. 5 and 10). Strike-slip faults bound the basin edges and largely encompass the Pliocene basin fill (Yaltırak, 2000a). For example, the thickness of young alluvial deposits is 1–2 m beyond the southwestern edge of the basin, thickening to 80 m just northeast of the basin-bounding fault (Yaltırak, 2000a).

4.2.4. Inegöl basin

The Inegöl Basin (IB) initially developed on the Thrace–Eskişehir Fault. It was uplifted and partially eroded during the Miocene under the control of strike-slip tectonics (Kaymakçı, 1991) (Figs. 5 and 10). More recently, these strike-slip faults were reactivated as normal faults by movement on the southern strand of the NAFZ, causing subsidence of the Inegöl Plain and IB to recommence.

4.2.5. Bursa Basin

The Bursa Basin (BB) overlies the Neogene Southern Marmara Basin (Figs. 4, 5 and 10). The dextral strike-slip fault outlining the northern boundary of the Yenişehir Basin crosses the southern part of the Bursa Plain (Figs. 5 and 10; Yaltırak, 2000a). The town of Bursa, Mount Uludağ and its slopes are situated on the alluvial fans developed in front of the normal faults parallel to this fault. Some normal faults, reactivated by the intersection of the southern strand of the NAFZ with the northwest–southeast-trending TEFZ, outline the eastern border of the triangular-shaped Bursa Plain (Figs. 5 and 10).

4.2.6. Manyas–Uluabat Basin

The Manyas–Uluabat Basin (M-UB) is superimposed on the Southern Marmara Basin and has developed under the control of the NAFZ (Fig. 4). The southern strands of the NAFZ to the south of the basin control modern sedimentation. This fault is made up of three segments. Its western and eastern segments exhibit strike-slip while the central part is a normal-oblique fault on which the Manyas and Uluabat Lakes have developed (Figs. 4, 5 and 10). Holocene alluvial deposits overlie Pliocene conglomerates at the margins of this wide plain with angular unconformity. To the north of the basin, between Karacabey and Bandırma, the boundary between the alluvial and Neogene deposits forms a distinct morphological step. Rivers that extend southward across this step have carved deep trenches. The M-UB has opened along normal faults with a dextral oblique component. These faults are located to the north and south of the basin.

4.2.7. Gönen Basin

The Gönen Basin (GB) developed where the middle and southern strands of the NAFZ became closest to each other (Figs. 4 and 10). Quaternary alluvium fills this fault-bounded basin, unconformably overlying folded Neogene rocks of the Southern Marmara Sub-basin. The basin developed here because of opening between the 'elbows' of the various fault strands, caused by southwestward bending of the southern strand of the NAFZ.

Fig. 10. Tectonic map of Marmara region (land area compiled from Ergül et al., 1986; Siyako et al., 1989; Yaltırak et al., 1998; Sakınç et al., 1999; Yaltırak and Alpar, 2002b; Alpar and Yaltırak, 2002 and field study). Faults on the map were identified on LANDSAT 5TM images and through field observations. Marine faults were mainly mapped using the shallow-penetration seismic lines of the Memorial University of Newfoundland. Not interpreted deep lines are from Okay et al. (1999, 2000); Siyako et al. (2000); Imren et al. (2001). Fault plane solutions are from Taymaz, (1990, 1999, 2000); Kalafat (1995), and Gürbüz et al. (2000). GPS vectors are plotted with respect to a fixed station at Istanbul (black star) (from Straub et al., 1997). Abbreviations: TEFZ, Thrace–Eskişehir Fault Zone; WMS-B, West Marmara Sub-basin; MMS-B, Middle Marmara Sub-basin; KS-B, Kumburgaz Sub-basin; EMS-B, Eastern Marmara Sub-basin; BS-B, Bandırma Sub-basin; GS-B, Gemlik Sub-basin; EHS-B, Eastern Hersek Sub-basin; ILB, Iznik Lake Basin; YB, Yenişehir Basin; INB, Inegöl Basin; BB, Bursa Basin; M-UB, Manyas–Uluabat Basin; GB, Gönen Basin.

5. Tectonic setting

As there are no detailed structural maps for the Marmara region, the exact location of the strands of the NAFZ on the land are not well established. The structural architecture of the region is compiled using existing 1:250 000 field maps, 1:500 000 satellite imagery, and digital topography maps (Figs. 5 and 10). This compilation revealed the presence of two different-aged systems in the Marmara Sea region, which intersect each other. The peculiar geometrical shapes of the Marmara Sea and the faults extending around its surroundings have clear differences in their orientation. The most important is the N45°W-trending TEFZ (Figs. 5 and 10). Others are the N80°E-oriented GFZ, the N45°E-oriented BBFZ and, parallel to this, the MEFZ (Figs. 5 and 10). With the exception of the TEFZ, these faults continue their activity controlled by the activity in the NAFZ. The splays of the TEFZ, which stay within the influence area of the NAFZ, play an active role in the evolution of the present geometry of the Marmara Sea.

5.1. Northwest Anatolia early neotectonic period (early Miocene–early Pliocene) fault systems

Early Miocene–early Pliocene faults in Northwest Anatolia include the dextral strike-slip TEFZ, which was active prior to the NAFZ, and its westward deflections, the GFZ, BBFZ and Edremit-Gönen Fault Zone (Figs. 5 and 10).

5.1.1. Thrace Eskişehir Fault Zone

At present, the TEFZ is dissected by the strands of the NAFZ and divided into four segments (Figs. 5, 9 and 11). Studies on the TEFZ in Eskişehir–Inönü (Gözler et al., 1985; Bozkurt, 2001), Inegöl (Kaymakçı, 1991), Bursa–Mudanya (Yaltırak, 2000a), and Thrace (Perinçek, 1991) define a major dextral strike-slip system which was active during the early Miocene–early Pliocene.

5.1.1.1. Eskişehir–Inegöl Segment

This segment of the TEFZ occurs between Bursa and Tuzgölü and is known under different names. Kaymakçı (1991) called the Inegöl Segment the 'Inegöl Fault Zone'. Altunel and Barka (1998) defined the Eskişehir Segment of the TEFZ as a normal fault. Bozkurt (2001) proposed that the TEFZ is a dextral normal fault developed during the Plio–Quaternary period. The Eskişehir–Inegöl segment is the longest segment (400 km) of the TEFZ, extending between the western part of the Tuzgölü and Bursa through Eskişehir (Fig. 11A,B). In many localities to the south, this fault segment is buried beneath Pliocene and Quaternary units. Around Tuzgölü, Eskişehir, Inönü, and Inegöl (Fig. 1A), Miocene dextral strike-slip faults later reactivated as normal faults creating Quaternary basins. This is also clearly visible on the Bouguer and magnetic maps prepared by MTA as well as on digital SAR interferometry topography maps (Fig. 11C,D).

5.1.1.2. Bursa–Mudanya Segment

This segment is ~48 km long and occurs between Bursa and Mudanya (Yaltırak and Alpar, 2002b). It exhibits characteristics of a normal fault and plays an important role throughout the evolution of the Bursa Plain (Figs. 5 and 10).

5.1.1.3. Imralı Segment

The Imralı segment is a ~62 km long, northwest–southeast-trending fault which occurs between Gemlik Bay and the Imralı Sub-basin. In Gemlik Bay, and between the eastern part of the Imralı Island and the MMS-B it displays characteristics of a normal fault (Figs. 5 and 10).

5.1.1.4. Adalar–Thrace Segment

This segment starts from Tuzla and extends to Thrace. It is the extension of the Imralı segment, which was offset by the northern strand of the NAFZ. It outlines the northern boundary of the EMS-B, where it displays normal sense separations (Figs. 6 and 10). Farther west, it loses its normal character and extends toward Thrace along the northern edge of the Central Marmara Trough, in the form of three parallel strike-slip zones (Figs. 5 and 10). The dextral strike-slip fault zone defined by a horsetail structure has initially been mapped by Perinçek (1991). At present, this structure, which is ~220 km long in East Thrace, and the northwest–southeast-trending zone is cov-

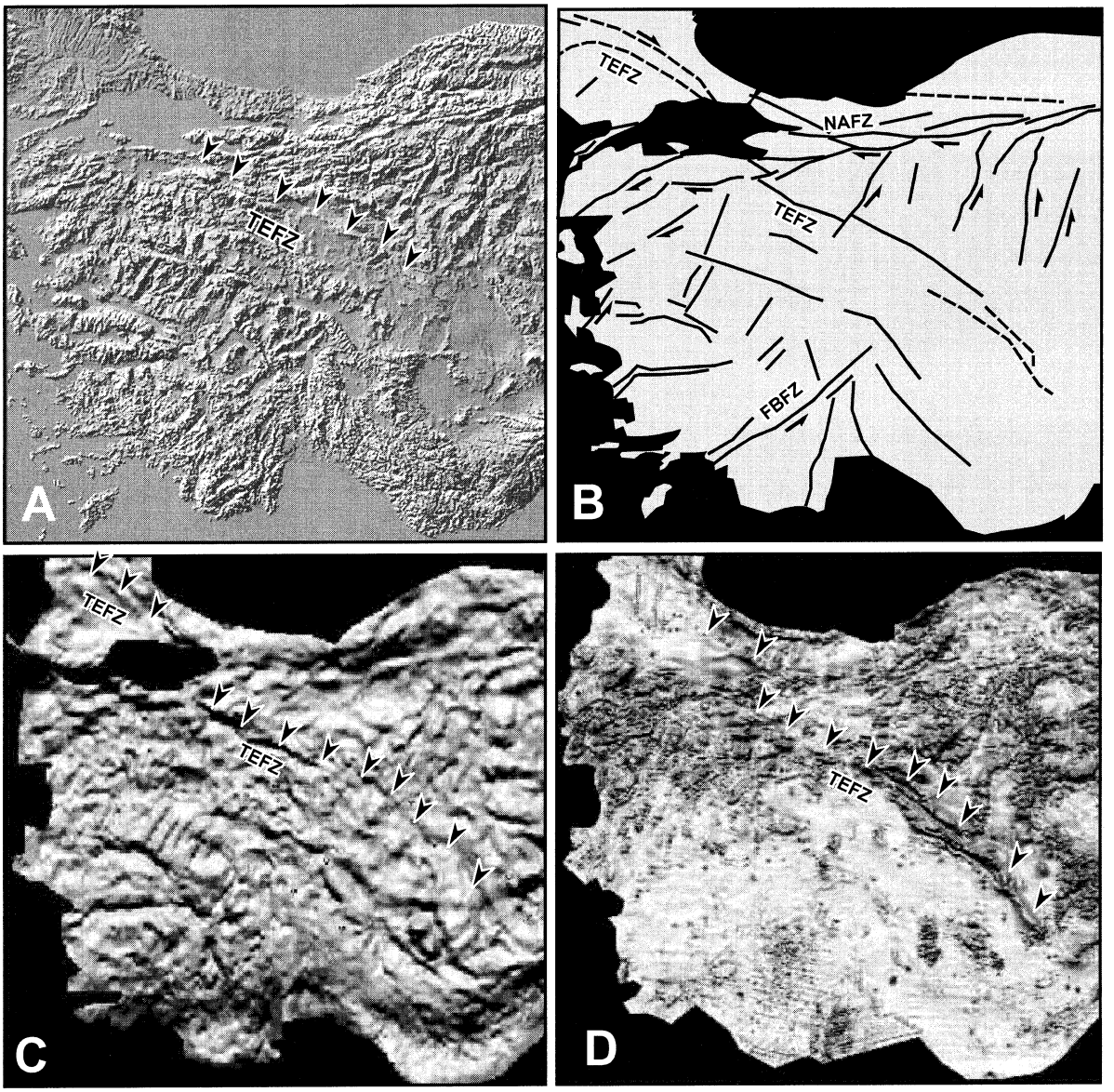

Fig. 11. (A) Digital elevation model map of West Turkey from Gazioğlu et al. (2002). Arrow shows TEFZ. (B) Main tectonic lines drawn from superimposed digital elevation model map, gravity and magnetic maps. Abbreviations: TEFZ, Thrace–Eskişehir Fault Zone; BFFZ, Burdur–Fethiye Fault Zone; NAFZ, North Anatolian Fault Zone. (C) Shaded Bouguer anomaly map of West Turkey (T = 20 km) from Akdoğan (2000). Arrow shows TEFZ. (D) Shaded total magnetic intensity map of West Turkey from Akdoğan (2000). Arrow shows TEFZ.

ered by Plio–Quaternary deposits (Figs. 5 and 10). This fault zone continues northward into Bulgaria, and one strand of it bends southward connecting with the Xanti–Kavala Fault in Greece (Tapırdamaz and Yaltırak, 1997).

5.1.2. Ganos Fault Zone

The GFZ starts from the KS-B and is composed of southward bending faults of the TEFZ (Figs. 5 and 10). It continues towards the North Aegean Trough. The GFZ is ~700 km long. To

the west, the south and north boundaries of the GFZ are the gently sloped normal faults defining the primitive structure of the Marmara Sea (Figs. 1, 5 and 6). Between these boundary faults, there are the northeast–southwest-trending WMR, the Ganos Mountain, Dolucatepe, Helvatepe, Anafartalar Thrust Fault, which are all located on the GFZ, occurring oblique to, and to the north and south of the master fault (Yaltırak and Alpar, 2002a). Westward, the GFZ joins the North Aegean system (Fig. 1B). In the present-day Gulf of Saros, the GFZ continues as a negative flower structure controlled by the master fault, with compression to the south, i.e. the Gelibolu Peninsula (Yaltırak et al., 1998, 2000a,b). The most distinguishing feature of this structure is its geometry. This V-shaped structure along the main fault composed of compressional and extensional blocks is similar to splays deviating from the master fault (e.g. the Yağmurlu–Ezinepazar Fault Zone and the Almus Fault Zone on the NAFZ; Bozkurt and Koçyiğit, 1996; Bozkurt, 2001).

5.1.3. Bandırma–Behramkale Fault Zone

The Bandırma–Behramkale Fault Zone (BBFZ) extends from the Bandırma Bay to the western part of Edremit Bay and is composed of a number of strike-slip faults of varying lengths (Figs. 1, 5 and 6; Siyako et al., 1989). This fault zone defines the interface between the Neogene units and the basement rocks to the south. Most of these segments are dextral and developed early Miocene–late Miocene depocentres dominated by local compression (Siyako et al., 1989). A net displacement of 8 km has been determined on a segment of this fault zone (see Inova–Sarıköy Fault; Siyako et al., 1989). Besides, there are 1–5 km offsets on other segments. It is highly possible that this system evolved as a fault bundle controlled by the internal deformations in the block to the south of TEF and GFZ.

5.1.4. Manyas-Edremit Fault Zone

The Manyas-Edremit Fault Zone (MEFZ) consists of *en echelon* faults, extending northeast–southwest from Gönen to Edremit Bay, within a 10–15-km-wide zone (Figs. 1, 5 and 6). It forms the interface between the Neogene units and the basement to its northwest. Many small-scale terrestrial basins have been developed along this dextral strike-slip fault. In one of these basins near Kalkım, the sediments intercalate with middle Miocene volcanic rocks forming a boundary between the faults and Neogene (Fig. 5). The layers of these deposits, which are folded and almost upright in position, imply that the activities of these faults even continued after the basin evolution.

5.2. Northwest Anatolia late neotectonic period (late Pliocene–Present) fault systems

The three strands of the NAFZ in the Eastern Marmara region came into existence in the late neotectonic period. These faults are superimposed on the early neotectonic fault systems.

5.2.1. Northern strand of the North Anatolian Fault Zone

The NAFNS starts from Bolu and reaches to the Eastern Marmara area through Izmit Bay (Fig. 1). In the Eastern Marmara Sea region, the NAFZ dips north and can be traced to the westernmost end of the EMT (Figs. 6, 9 and 12). Further west, the NAFNS is connected to GFZ of the EMR within an ~10-km wide region (Figs. 7, 9 and 12). The EMR is a typical restraining band, similar to those observed in dextral strike-slip systems (Sylvester, 1988; Ben-Avraham, 1992). The oblique tension developed between the Adalar Fault Zone, the northern boundary of the EMT. The oblique extension between the Adalar Fault Zone, extending north of the EMT, and the North Anatolian Fault caused the opening of the EMS-B. Because the GFZ crosses the MMT obliquely southward the oblique compression caused the development of the ENE–WSW-trending MMR. Because the GFZ changes its direction westward, WNW–ESE-trending normal faults created the MMS-B (Figs. 7, 8, 10 and 12). Further west, the GFZ, trends westward, causing the development of the northeast–southwest-trending WMR (Figs. 7, 8, 10 and 12). This typical push-up is controlled by the thrust faults developed at an angular to the

right-lateral movement (Sylvester, 1988). To the west of the WMR, the BMS-B opened as the result of a north–south extension created by the bending associated with compression in the GFZ (Figs. 7, 10 and 12). Further west, GFZ extends to the Northern Aegean Sea crossing a land bridge (Figs. 1 and 10). At present, in the central and western Marmara Sea region, the sub-basins and ridges continue their evolution in a tectonic regime superimposed on the negative flower structure created by the GFZ (Figs. 6, 9, 12 and 13). Further east, due to intersection of the TEFZ and the NAFZ, the Thrace–Eskişehir fault trending 45° oblique to the NAFZ (i.e. Adalar and Imrali Fault Zones) gains activity created by the extensional regime consistent with the right-lateral strike-slip systems. These faults were converted into normal faults (Fig. 10). Thus, the GFZ and the northern strand of the NAFZ are connected to each other under the CMR, which will transmit the dextral movement further (Fig. 13). The consequence of the NAFZ reaching the Marmara region in late neotectonic period and propagating towards the GFZ, the NAFNS formed a deep and single structure beneath the EMR, connecting the two segments of the master fault in the western and eastern Marmara in a single structure at depth.

5.2.2. *Middle strand of the North Anatolian Fault Zone*

The North Anatolian Fault bifurcates in Bolu. Then it again bifurcates around Pamukova or Geyve (Figs. 1 and 10; Koçyiğit, 1998). The middle strand, which extends to Gemlik Bay via Pamukova and Iznik Lake, intersects with the TEF, causing the opening of the Gemlik pull-apart basin. The reactivated segments of TEF caused the deepening of this basin (Yaltırak and Alpar, 2002b). At present, the middle strand follows the coastal line from Gemlik Bay to Bandırma Bay and it deflects 20° southward into Bandırma Bay. The main reason for this deflection is its connection with the BBFZ (Figs. 5, 9 and 13). At present, the BBFZ continues its activity as a middle strand of the NAFZ, the NAFMS, similar to the GFZ at the western Marmara Sea.

5.2.3. *Southern strand of the North Anatolian Fault Zone*

The NAFSS follows the southern boundary of the Yenişehir Basin (Fig. 10). Further west, the movement is transferred into a fault situated to the north of the Inegöl Basin, and the southern strand intersects the TEF for the third time east of Bursa (Figs. 5 and 10). The NAFSS outlines the southern boundary of the Bursa Plain, and then follows the southern margins of Uluabat and Manyas Lakes. The block that deflects southward due to compression causes an oblique tensional regime between Manyas and Uluabat (Figs. 5 and 10). The southern strand extends into Edremit Bay via the MEFZ, with a progressively reduced rate of motion.

6. Regional seismicity

Many historical earthquakes with magnitudes >7 are known to have occurred within the study area (Ambraseys and Jackson, 2000). Fault plane solutions of the earthquakes considered in this study show the effective deformation responsible for the opening and evolution of the Marmara basins and are in good agreement with the observed faults.

6.1. *Earthquakes on the northern strand of the North Anatolian Fault*

These earthquakes occurred on east–west-trending strike-slip faults dominantly dextral in sense with 6.6–7.4 M_s and $\sim$10 km focus depth. Starting from the east, these are the 1943 Hendek, 1951 Kurşunlu, 1957 Abant, 1967 Mudurnusuyu–Adapazarı, 1999 Izmit, and 1999 Düzce earthquakes (Mc Kenzie, 1972; Ambraseys and Jackson, 1998; Taymaz et al., 1991, 2001; Taymaz, 1999, 2000). The earthquakes with magnitudes <6.4 occurring in the Marmara Sea have different characteristics from the above. In particular, distributions of earthquakes measured at local stations since 1997 and the focal mechanism solutions of the aftershocks of the 1999 Izmit earthquake (Ergin et al., 2000) give kinematic clues for the Marmara faults (Fig. 10). The biggest of the

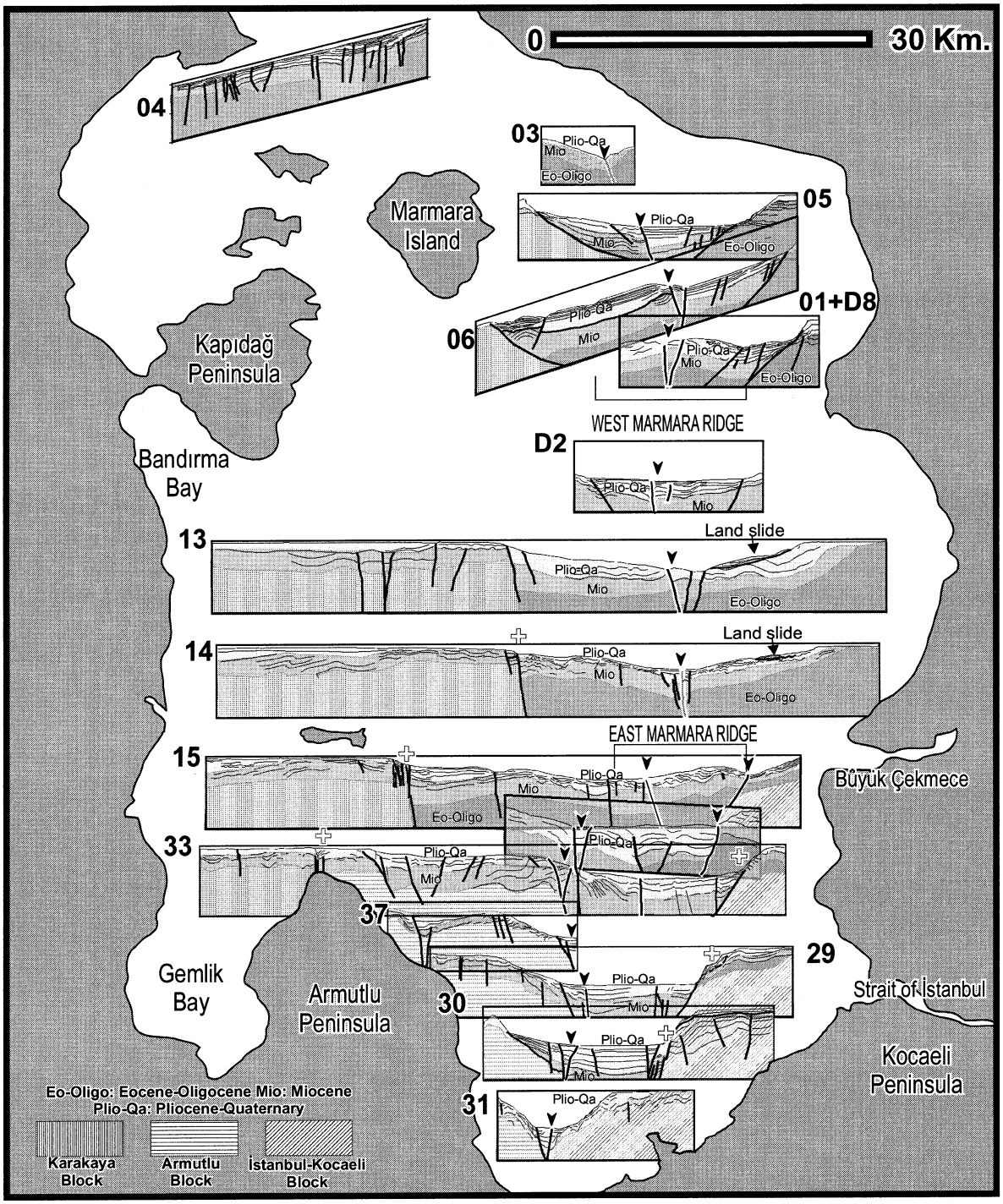

Fig. 12. Structural block diagram of the Marmara Sea composed from seismic lines re-interpreted in this paper (Fig. 6).

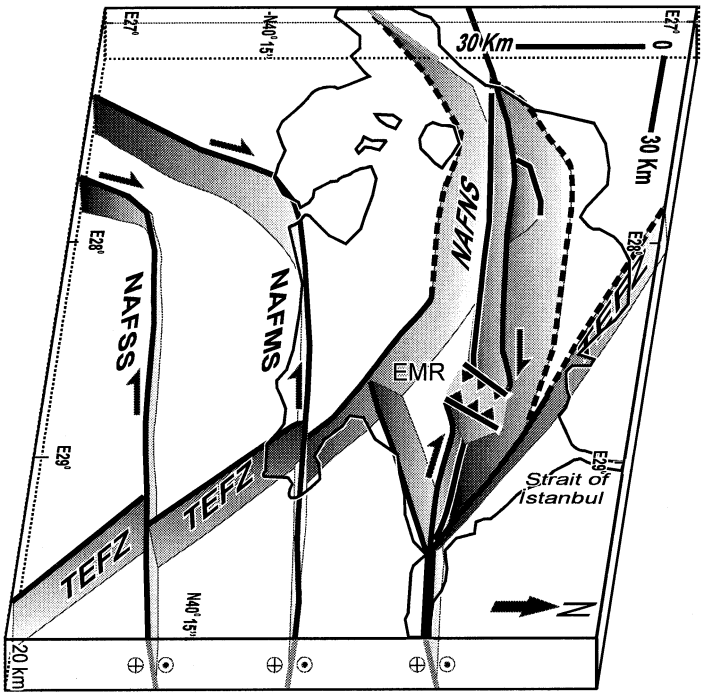

Fig. 13. Structural model block diagram of the Marmara region faults. This figure shows the linkages between the Thrace–Eskisehir Fault parts and the North Anatolian Fault segments. Abbreviations: TEFZ, Thrace–Eskişehir Fault Zone; NAFNS, North Anatolian Fault North Segment, i.e. 'Great Marmara Fault' of Le Pichon et al. (1999); NAFMS, North Anatolian Fault Middle Segment; NAFSS, North Anatolian Fault South Segment.

earthquakes in the Marmara region occurred in the Adalar Fault Zone in 1963. Its fault plane solution indicates a northwest–southeast-trending extension along normal faults (Taymaz, 1990, 2000). Here, the northwest–southeast-trending normal faults form the northern boundary of the EMT (Fig. 10). It is important to note that the aftershocks of the 1999 earthquakes (Ergin et al., 2000) are stacked along the margins of the EMT, possibly caused by the splitting of the fault into two branches. Comparison of the aftershock distribution with the fault map of Ergin et al. (2000), Alpar and Yaltırak (2002) have suggested that the trends in the aftershocks are a production of deformation scattered at the end of the fault of the 1999 Izmit earthquake, which terminated around the eastern end of the EMT. The tectonic setting proposed by Alpar and Yaltırak (2002) and fault plane solutions reflect the character of a dextral strike-slip deformation at the margins of the EMS-B. The results of a seismographs network operated before the 1999 earthquakes obviously indicate a series of earthquakes also corresponding with the deep Marmara troughs (Fig. 10; Gürbüz et al., 2000). On this line, there are two earthquakes focused to the south of the EMT. The eastern earthquake revealed a northwest–southeast-oriented normal right-lateral oblique solutions, while the second earthquake, which is located to the central west of the EMT, gave a northeast–southwest minor compression (Fig. 10). The fault plane solution of another earthquake on the EMR also indicated compression with a minor right-lateral component. This fault, along which these three earthquakes are aligned, extends from the Izmit Bay to the EMR and dips northward (Figs. 9, 12 and 13).

Fault plane solutions for earthquakes along the fault extending between the KT and the MMT give northeast–southwest-oriented strike-slip with varying extension as well as northwest–southeast-directed extension that can be correlated with nor-

mal faults in the region (Gürbüz et al., 2000). In the central part of the MMT, the master fault passes through the central portion of the trough reaching the WMR. Here, the fault plane solutions show strike-slip with extension (Fig. 10). The fault plane solution for the earthquake located on a thrust fault between the WMT and WMR (Fig. 10; Gürbüz et al., 2000) show northeast–southwest compression. All these earthquakes have their focal depth <15 km (Gürbüz et al., 2000). There are few fault plane solutions for the western part of the Marmara region on the NAFNS. One of them gives northeast–southwest-directed compression, possibly correlating with a similar trending trust fault on the GFZ around Ganos Mountain (Fig. 10; Kalafat, 1995). Dextral strike-slip offsets of <5.5 m observed between Gaziköy and the Gulf of Saros developed as the results of the 1912 Şarköy–Mürefte earthquake (Altunel et al., 2000; Altınok et al., 2001). Detailed field observations conducted on the GFZ closer to the Marmara Sea indicated the presence of northeast–southwest-trending thrust faults oblique to the master fault (Yaltırak, 1996).

The fault plane solutions of an earthquake which occurred in 1975 on the northern strand of the NAFZ extending along the northern margin of the Saros Trough (Yaltırak and Alpar, 2002a) gave right-lateral offset with normal component (Fig. 10; Taymaz, 1990, 2000).

6.2. Earthquakes on the middle strand of the North Anatolian Fault

No large earthquakes have been recorded on the middle strand of the NAFZ and its eastern extension during the period when seismographic data were available. However, there is a dense seismic activity around Gemlik and Bandırma Bays (Fig. 1B). Gürbüz et al. (2000), identified seven small earthquakes between Iznik Lake and the Southeast Marmara Sea (Fig. 10). Fault plane solution of earthquakes located north of Iznik lake give northwest–southeast-trending extension along normal faults, whereas those closer to the Armutlu Peninsula give northeast–southwest dextral strike-slip.

Fault plane solutions of Gürbüz et al. (2000) for Gemlik Bay are consistent with the oblique normal faults observed in the seismic reflection profiles (Fig. 10). Although there is no earthquake west of the middle strand of the NAF, three of fault plane solutions given by Gürbüz et al. (2000) on land are close to the master fault (Fig. 10), and show dextral strike-slip character (Fig. 10). In addition, fault plane solutions of the 1953 and 1969 Yenice earthquakes on the eastern part of the middle strand give northeast–southwest-trending thrust faults with right-lateral component and pure dextral strike-slip faults, respectively (Fig. 10; Taymaz, 1990, 2000), consistent with the southward bending of the middle strand and westward escape of the Anatolian Block.

6.3. Earthquakes on the southern strand of the North Anatolian Fault

On the southern strand of the North Anatolian Fault the largest earthquakes throughout the period when seismographic data were available are the 1964 Manyas and the 1983 Yenişehir earthquakes (Ketin, 1966; Taymaz, 1990). Different epicentres have been proposed for the 1983 earthquake (Taymaz, 1999; Gürbüz et al., 2000). However, fault trends for either solutions are in the same direction with the southern strand of the North Anatolian Fault (Fig. 10).

Around Bursa, the fault plane solutions of Gürbüz et al. (2000) give different fault directions consistent to the geometry the intersection of the NAFSS and TEFZ (Figs. 1B and 10). The 1964 Manyas earthquake is another event related to the southern strand, giving an almost east–west-trending normal fault plane solution (Fig. 10; Taymaz, 1990). Although its epicentre is placed to the north of the Uluabat–Manyas Basin (Taymaz, 1990), detailed field surveys conducted after the earthquake along the fault rupture placed it to the south of the basin indicated surface deformations associated with a dextral strike-slip fault (Ketin, 1966, 1969). The NAFSS bends 45° south starting at the town of Gönen and turns a transfer zone compressed by 'echelon' faults (Fig. 10). The fault plane solution of the 1971 earthquake at the western extension of this fault, gives northeast–southwest-trending compression along thrust

faults, oriented dominated by the right-lateral strike-slip component (Fig. 10; Gürbüz et al., 2000).

7. Offsets of the strands of the North Anatolian Fault in the Eastern Marmara region

Until recently the amounts displacement on the strands of the NAFZ could not be precisely determined, thus estimates of total displacements ranged from 20 to 85 km (e.g. Bozkurt, 2001). Detailed measurements can now be made by combining GPS vectors, digital topographic maps compiled using SAR interferometry, and marine seismic profiles.

Due to the digital topography map prepared by Wright et al. (2001) and SAR interferometry the relation of the strands of the NAFZ with the TEFZ can be evaluated in the region of Bursa (Fig. 14), as well as the Sakarya River, which has been offset by the NAFZ at two sites: south of Düzce Plain and Pamukova where the NAFZ bifurcates (Fig. 14). The digital topography map shows that the Sakarya River is offset by the NAFNS ~58 km from its older riverbed to the north (Fig. 14). However, a ~18-km displacement is observed at Pamukova where it is cut through by the NAFZ (Koçyiğit, 1988). The TEF is also cut through by the southern strand of NAFZ by ~10–11 km (Fig. 14).

Alpar and Yaltırak (2002) used seismic reflection data to calculate the displacement of the TEF by the middle strand of the NAFZ in Gemlik Bay as 7–8 km (Fig. 14). The total of the Bursa and Gemlik offsets are almost exactly 18 km on the digital topographical map. In the Marmara Sea, there is 56–63-km offset between the segments of the TEF cut by the northern strand of the NAFZ (Fig. 6), which is consistent with the 58-km offset observed on the Sakarya River (Fig. 14). The other way controlling the offsets on the NAFZ obtained by seismic data is the calculation based on age determination of the discontinuity between the end of the early Pliocene and late Pliocene, as caused by the activity of the NAFZ, by using GPS slip vectors. This discontinuity corresponds to 3.4–3.7 Ma (Yaltırak et al., 2000a). Using the GPS slip vectors (Straub et al., 1997) the relative displacements during the last 3.5 Ma between the blocks are calculated as 59.5 km along the NAFNS (average velocity 17 mm/yr), as 7.4 km along the NAFMS (average velocity 2.1 mm/yr) and as 10.5 km along the NAFSS (average velocity 3 mm/yr). Hence, the displacements of the strands of the NAFZ around the Marmara Sea region are 58–59, 7–8, and 10–11 km, on the northern, middle, and southern branches, respectively. These figures indicate a total of 75–78-km total displacement in the region, which is consistent with the 85 ± 5-km and 80-km displacements calculated by Şengör (1979) and Hubert-Ferrari (1998) for the central and eastern parts of the NAFZ, respectively. The highest westward escape of the Anatolian Block is along the northern strand (77%), followed by southern (14%) and middle (9%) strands.

8. Geological evolution of the Marmara Sea region using palinspastic modelling

Palinspastic maps were prepared using fault plane solutions and GPS slip vectors representing each block defined by the strands of the NAFZ (Fig. 15). On these maps, the city of Istanbul is assumed to be a fixed base point, the blocks were then simultaneously moved for every 500 000 yr.

The TEFZ and its spalys were in the Marmara region ~4 Ma (Fig. 15A). Four blocks located to the west of the TEFZ (TB, MB, GB, and BB) were separated from each other by the dextral GFZ, BBFZ and MEFZ. While to the east of the TEFZ, the Thrace Armutlu Block extended towards Anatolia (Fig. 15A). When the NAFZ reached the eastern Marmara region ~3.5 Ma, it cut through the TEFZ at three locations, ceasing the activity of the TEFZ in Thrace. However, the GFZ, BBFZ and MEFZ were incorporated into the NAFZ, and thus continued their activity. During this period, the northwest–southeast-trending segments of the TEFZ were reactivated as normal faults (Fig. 15B). The EMS-B started to evolve due to segmentation of the TEF resulting from the first offset along the nascent NAFZ, which activates as a boundary of TKB between

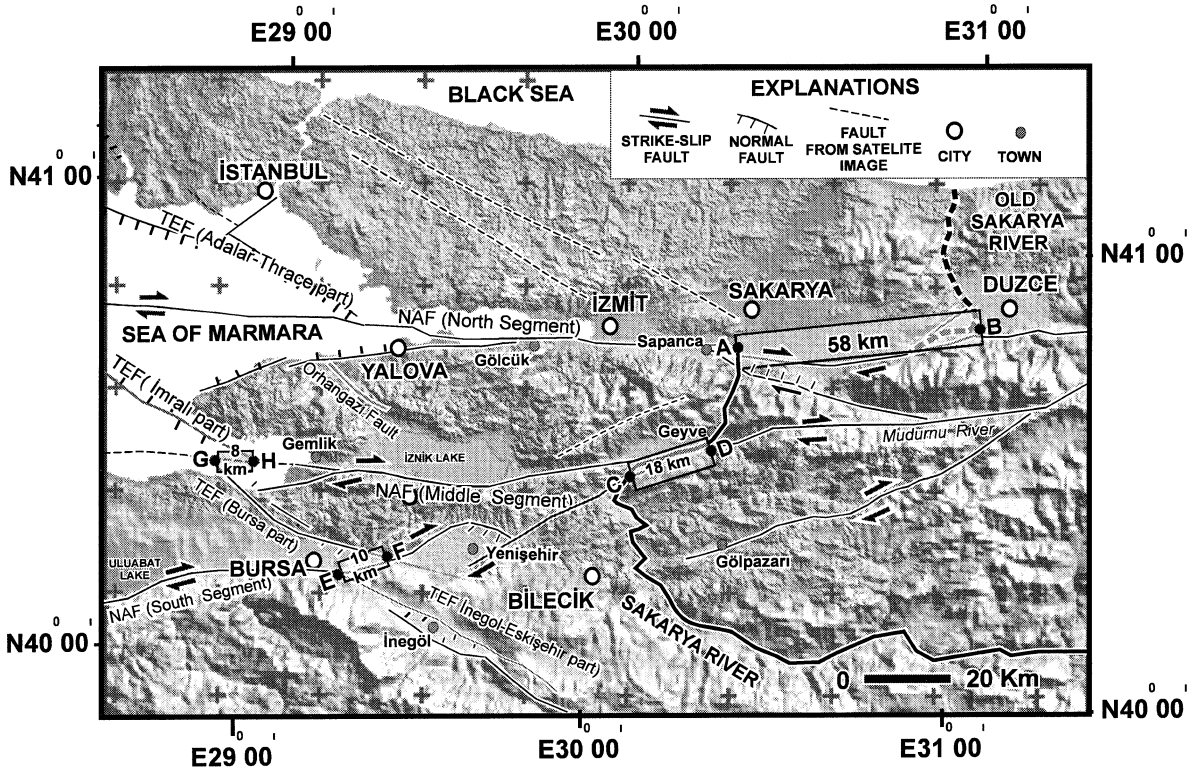

Fig. 14. Morphotectonic map of the East Marmara region. Faults from Yaltırak (2001a), Alpar and Yaltırak (2002), Yaltırak and Alpar (2002b). Digital elevation map from Wright et al. (2001). Shaded rectangle shows total displacement on the NAFZ segments. This study used by indicator TEFZ and Sakarya River for displacement. A–B: Sakarya River 58 km displaced by NAFZ. C–D: Sakarya River in Pamukova, 18 km displaced by NAFZ. C–D = E–F: TEFZ in Bursa, 10 km displaced by NAFZ). G–H: TEFZ in Gemlik, 8 km displaced by NAFZ.

the NAFNS and GFZ (Fig. 15B). During this period the Ganos region and the Gaziköy–Gelibolu areas started to uplift (Fig. 15A). The GFZ and the eastern parts of the NAFZ in the Eastern Marmara Sea define the northern boundary of the Marmara Block which continued its westward escape 3–2.5 Ma ago (Fig. 15B–D). The step between these two faults first caused the evolution of the EMS-B, but later, the EMR started to uplift by the stretching of the northeast margin and squeezing of the western parts (Fig. 15E–G). To the west the Gaziköy–Gelibolu uplift abandoned the MMS-B and placed it to the south of WMS-B (Fig. 15D,E,G). During this period, the Marmara Basin started to evolve superimposed on the GMS-B (Fig. 4). Simultaneously, some of the right-lateral faults with thrust components developed on the negative flower structure by the GFZ. While the Eastern Marmara part of the NAFZ progressed westward, EMR started to uplift and rotate clockwise (Fig. 15E–J). While westward escape of the Anatolian Block resulted compressional forces on the eastern and central Marmara ridges, causing their uplift, some thrusts oriented 45° oblique to the master fault were developed in the western Marmara area. Meanwhile in the southern Marmara region the Imralı Sub-basin, together with the EMS-B, continued its evolution in front of the TEF segment which was reactivated as a normal fault (Fig. 15B–J).

Another important feature revealed by the palinspastic maps is the degree of the north–south extension. During the last 2.5 Ma, the southern coast of the Marmara Sea separated from the northern coast 2 km in north–south direction and 42 km in west–east direction, implying that

the dominant movement responsible for the evolution of the Marmara Sea is strike-slip.

9. Discussion

All models proposed for the evolution of the Marmara Sea are largely based on marine seismic profiles, with limited land data (Barka and Kadinky-Cade, 1988; Wong et al., 1995; Ergün and Özel, 1995; Barka, 1992; Parke et al., 1999; Siyako et al., 2000; Okay et al., 2000; Le Pichon et al., 1999; Aksu et al., 2000; Imren et al., 2001). Thus, these studies failed to provide a comprehensive tectonic model for the evolution of the Marmara region. The common point of these studies is the assumption that the NAFZ is an unique element responsible for the development of structures in the Marmara region. Yaltırak (2000b) showed that faults on land that are older than NAFZ, such as the TEFZ, GFZ, BBFZ, and MEFZ, were active in the western Marmara area as early as the early Miocene, and that basins formed in relationship to these faults shaped the area before the NAFZ, or the 'neotectonic period' as defined by Şengör (1980). This early neotectonic period includes the evolution of the TEFZ and its splays and the development of Northwest Anatolia in early Miocene–early Pliocene to Recent times. The suggestion of Perinçek (1991) that the TEFZ was the continuation of the NAFZ requires an impossible kinematic model, requiring the 45° clockwise rotation of the Anatolian Block to trend northward. Paleomagnetic data on Thrace giving counterclockwise rotations do not support this interpretation (Tapırdamaz and Yaltırak, 1997). Similarly, the TTT-triple junction model proposed by Okay et al. (2000), correlating the evolution of the northwest–southeast-trending inactive strike-slip faults on the Thrace with the NAFZ, also poses a kinematic impossibility. Here the central block in the Marmara Sea is proposed to escape westward. The westward escape of the Anatolian Block does not require the north and south branches of the NAFZ, particularly in the presence of the GFZ. If this model were true, an northeast–southwest extension would be needed on the Thrace–Eskişehir Fault Zone, which should also display as much offset as that observed on the NAFZ. However, seismic reflection profiles from Thrace does not show the presence of a deep graben structure filled with young sediments (Perinçek, 1991), thus does not corroborate with this interpretation. The gravity, magnetic and seismic data as well as detailed field studies clearly document that the Thrace–Eskişehir Fault Zone in Thrace and Anatolia is a a huge structure that was not created by the NAFZ.

The age of the North Anatolian Fault has been discussed by many researchers (Ketin, 1948, 1969; McKenzie, 1972; Şengör, 1979; Barka, 1992; Barka et al., 2000; Barka and Kadinky-Cade, 1988; Koçyiğit, 1988, 1989, 1991; Şaroğlu, 1988; Toprak, 1988; Barka and Gülen, 1989; Bozkurt and Koçyiğit, 1996; Yaltırak, 1996; Okay et al., 1999, 2000; Tüysüz et al., 1998; Yaltırak et al., 2000a,b, 1998). Some of the recent studies proposed that it has been active for the last 5 Ma (Koçyiğit, 1988, 1989, 1991; Şaroğlu, 1988; Toprak, 1988; Bozkurt and Koçyiğit, 1996; Yaltırak, 1996; Tüysüz et al., 1998). However stratigraphic studies around the Marmara Sea region suggest an age of 3.5 Ma (Yaltırak et al., 1998; 2000a,b; Sakınç et al., 1999; Alpar and Yaltırak, 2002; Yaltırak and Alpar, 2002a,b). This younger age is corroborated by the arguments put forward in this study; e.g. the relation between the TEFZ and NAFZ, regional stratigraphy, palinspastic maps reconstructed from development history of the sub-basins. The initiation of the NAFZ is ultimately related to the near-constant opening of the Red Sea and the Gulf of Aden during the last 4 Ma (Chu and Gordon, 1998; Dauteuil et al., 2000). In addition, the studies on the Dead Sea Fault in Syria indicated that the Ghab Basin started its evolution in Early Pliocene (4.5 Ma) (Brew et al., 2001). The ~4-Ma age is probably the maximum age for the NAFZ at its easternmost termination: we expect that it is younger in western Anatolia. For example, Ünay et al. (2001) obtained an age of late Pliocene (2 Ma) from deposits in front of a normal fault with dextral oblique component placed between the two strands of the North Anatolian Fault (see also Fig. 14; the northwest–southeast-oriented fault between Sapanca and Mudurnu).

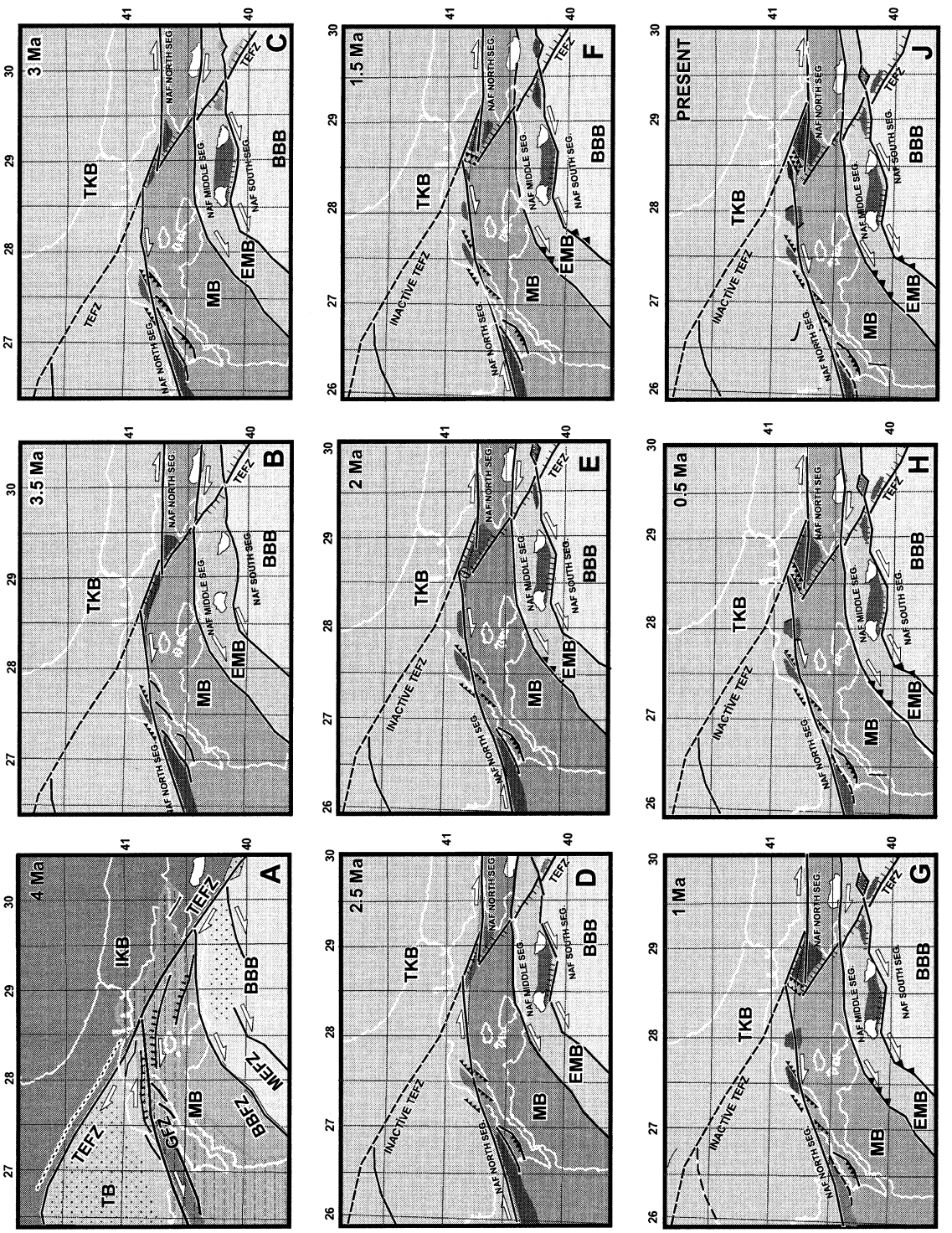
4 Ma
A
TEFZ
IKB
TB
GFZ
MB
BBFZ
MEFZ
BBB
3.5 Ma
B
TKB
NAF NORTH SEG.
NAF MIDDLE SEG.
NAF SOUTH SEG.
EMB
3 Ma
C
2.5 Ma
D
INACTIVE TEFZ
2 Ma
E
1.5 Ma
F
1 Ma
G
0.5 Ma
H
PRESENT
J
26
27
28
29
30
40
41

This late Pliocene age implies that the faults oblique to the North Anatolian Fault are younger than the main system and the basins along the North Anatolian Fault and its surrounding are also younger than 3.5 Ma.

During the last 3.5 Ma the NAFZ reactivated some of the northwest–southeast-trending older faults associated with TEFZ in Northwest Anatolia, by inverting them as normal faults, causing the development of several basins. Several young basins developed associated with the NAFZ became superimposed with these older basins. The structures observed on the marine seismic data illustrate this superimposed geological history.

It is necessary to distinguish the structures west and east of the EMR. The western and central Marmara regions are characterised by a negative flower structure. The EMR was formed as the northern strand of the NAFZ crossed the southern boundary of the EMT to the GFZ to the north. It is believed that faults interpreted as two separate segments by Okay et al. (2000) and Siyako et al. (2000) south and north of the EMR must be connected by a master at depth. Because the focal depths of the earthquakes along the NAFZ occur at ~10–20 km, the deep faults interpreted as separate segments by Okay et al. (2000) and Siyako et al. (2000) south and north of the EMR probably correspond to a single buried master fault. Although in principle the single fault models proposed by Le Pichon et al. (1999), Aksu et al. (2000), and Imren et al. (2001) are correct, but incomplete because they do not take into account the structures associated with the early and late neotectonic periods. In the *en echelon* fault models Parke et al. (1999), Okay et al. (2000) and Siyako et al. (2000) explain the kinematic evolution of the region by a series of separate fault segments. But, they ignore that narrowing amount between the segments would be much higher in case the fault activates in segments.

The lateral offset along the North Anatolian Fault varies between 20 and 85 km (e.g. Ketin, 1948, 1969; Şengör, 1979; Şengör et al., 1985; Armijo et al., 1999; Bozkurt, 2001). In this study, the offset along the North Anatolian Fault is calculated as 75–78 km.

10. Conclusion

The Marmara region is a superimposed structure, which was formed by two different fault systems during two different periods. These structures are the TEFZ and its splays in the early neotectonic period and the NAFZ and its strands in the late neotectonic period. The total offset of the NAFZ in the Marmara Sea is ~75–78 km.

During its westward escape at 22 mm per yr, the Anatolian Block causes 59, 7–8, and 10–11 km lateral offsets on the northern, middle, and southern strands of the NAFZ, respectively. The ratios of the westward escape of the Anatolian Block are 77, 9, and 14% along the northern strand, middle, and southern branches, respectively. The NAFNS is an almost east–west-trending arc-shaped fault which is buried only under the EMR. Westward, it reaches to the Gulf of Saros via the GFZ. The middle strand changes its westward trend by bending southward at Bandırma. On these areas, it has thrust component and right-lateral character. The M-UB developed on the extensional region caused by the southward bending of the southern strand at Manyas. While the Yenişehir Basin opens as a typical pull-apart basin due to northeast–southwest extensional regime, the M-UB opens due to the north–south extensional regime, because the Balıkesir–Bursa Block to its south escapes southward. The fault plane solu-

Fig. 15. Palinspastic palaeogeographic reconstruction maps showing Plio–Quaternary tectonic evolution of the Marmara region. The palinspastic maps have been prepared for every 500 000 yr on the basis of regional GPS vectors given by Straub et al. (1997). (Fig. 10 shows GPS vector.) The city of Istanbul was held constant and each block was reconstructed backward on the basis of the boundary faults and GPS vectors. Abbreviations: IKB, Istanbul–Kocaeli Block; TB, Thrace Block; TKB, Thrace–Kocaeli Block; MB, Marmara Block; EMB, Edremit–Manyas Block; BBB, Bursa–Balıkesir Block; TEFZ, Thrace–Eskişehir Fault Zone; GFZ, Ganos Fault Zone; BBFZ, Bandırma–Behramkale Fault Zone; MEFZ, Manyas–Edremit Fault Zone; NAF, North Anatolian Faults

tions obtained in the Marmara Sea region are in good agreement with the faults proposed in this study.

All of the basins in the Marmara region opened by the NAFZ have the features of the early neotectonic period. Therefore, even while each of these basins opened due to different tectonic processes, they are consistent with each other within the frame of the regional tectonic picture. The pull-apart geometry of the Gemlik and Yenişehir Basins show different features. It is not possible to suggest that a north–south extensional regime existed in the Marmara region just looking to the features of the Uluabat–Manyas Basin. In addition, one can not interpret NE-SW trending strike-slip faults similarly just looking to the features of the Yenişehir Basin or one cannot claim compression just looking to the compressional areas where the middle and southern strands of the NAFZ bend southward.

The shaping of the Marmara Sea is still continuing under the compressional forces in the Western Marmara (Gelibolu–Biga Peninsula) caused by to northwest–southeast right-lateral shearing mechanism and the north–south extensional forces between Bandırma and Bursa. The ridges and compressional troughs in the central Marmara Sea developed due to the jumps between the fault segments. The normal faults bounding the Marmara shelves, which started their activities in the early neotectonic period and are also known as the northern and southern boundary faults, can be still active as normal faults due to existing rotational extensions (1–2 km) between the blocks.

It is impossible to relate all of the structures in the Marmara Sea region to the NAFZ genetically and to assume that the North Anatolian Fault created everything. As a result, the proposed evolution models are forced to define the evolution of the region by the same tectonic regime. The main result of this study is a new synthesis based on the combination of data presented in previous works. Therefore, this synthesis confirms all of the data presented in previous works, but it does not confirm all of the previous tectonic models proposed for the evolution of the Marmara Sea.

Acknowledgements

This paper was written when the author was a visiting scientist at the Memorial University of Newfoundland. Research funds are acknowledged from the Natural Sciences and Engineering Research Council of Canada (Marmara Sea Gateway Project). Thanks are due to Aksu, Hiscott and Calon for the shallow Seismic Lines. The author is also indebted to Mehmet Sakınç, Fazlı Y. Oktay and Cengiz Tapırdamaz, who have accompanied his studies in the Marmara Sea region since 1990 and contributed to the results presented here. Further thanks are due to Bedri Alpar, who was the first researcher suggesting the author to combine marine geological and geophysical data with those observed on land and his immense data sets of shallow seismic data collected mainly after the 1999 earthquake. Thanks are due also to the *Marine Geology* reviewers Jeremy Hall and Erdin Bozkurt for their helpful suggestions and to Aral Okay who was the first to propose the study on the GFZ, leading to this paper, and provided conventional seismic sections collected by the MTA. Finally, the author likes to thank his wife Kezban Saki-Yaltırak, who is responsible for the C.E.P. Foundation, which sponsored all his investigations.

References

Akdoğan, N., 2000. Türkiye magnetik-gravimetrik çizgisellikleriyle neotetis paleotektonik üniteleri çizgiselliklerinin korelasyonu ve bazi sonuçlar. Cumhuriyetin 75. Yildonumu Yerbilimleri ve Madencilik Kongresi MTA, Ankara, pp. 331–345.

Aksu, A.E., Hiscott, R.N., Yaşar, D., 1999. Oscillating Quaternary water levels of the Marmara Sea and vigorous outflow into the Aegean Sea from the Marmara Sea-Black Sea drainage corridor. Mar. Geol. 153, 275–302.

Aksu, A.E., Calon, T.J., Hiscott, R.N., Yaşar, D., 2000. Anatomy of the North Anatolian fault zone in the Marmara Sea. Western Turkey: Extensional basins above a continental transform. GSA Today 10, 1–2.

Alpar, B., Yaltırak, C., 2000. Çınarcık Çukuru ve çevresinin morfotektoniği. In: Uysal, Z., Salihoğlu, I. (Eds.), 1. Ulusal Deniz Bilimleri Konferansı, 30 Mayıs–2 Haziran 2000, ODTÜ, Erdemli Deniz Bilimleri Enstitüsü ve TÜBITAK, Bildiri ve Poster Özetleri. ODTÜ, Ankara, pp. 189–194.

Alpar, B., Yaltırak, C., 2002. Characteristic features of the

North Anatolian Fault in the Eastern Marmara region and its tectonic evolution. Mar. Geol. 190, S0025-3227(02)00353-5.

Altınok, Y., Alpar, B. Yaltırak, C., 2001. Tsunami of the 1912 Earthquake (Ms = 7.4), extension of the associated faulting in the Marmara Sea. NATO Advanced Research Workshop On 'Underwater Ground Failures on Tsunami Generation, Modeling, Risk and Mitigation', May 23–25, 2001, Istanbul.

Altunel, E., Barka, A.A., 1998. Neotectonic activity of Eskişehir fault zone between Inönü and Sultandere. Geol. Bull. Turk. 41, 41–52.

Altunel, E., Barka, A.A., Akyüz, H.S., 2000. Slip distribution along the 1912 Murefte-Şarköy earthquake, North Anatolian Fault, Western Turkey. In: Barka, A.A., Kozacı, Ö., Akyüz, S.H., Altunel, E. (Eds.), 1999 Izmit-Düzce Earthquakes: Preliminary Results. Istanbul Technical University Publ., pp. 341–349.

Ambraseys, N.N., Jackson, J.A.., 1998. Faulting associated with historical and recent earthquakes in the Eastern Mediterranean region. Geophys. J. Int. 133, 340–406.

Ambraseys, N.N., Jackson, J.A., 2000. Seismicity of the Sea of Marmara (Turkey) since 1500. Geophys. J. Int. 141, F1–F6.

Andrussov, N., 1890. Die Schichten von Cap Tschauda. Ann. der K.K. Naturhistor. Hofmuseums, Wien 5, 66–76.

Ardel, A., Kurter, A., 1973. Marmara Denizi. I. Ü. Coğraf. Derg. 18–19, 57–75.

Armijo, R., Meyer, B., Barka, A.A., Hubert, A., 1999. Propagation of the North Anatolian fault into the Northern Aegean: timing and kinematics. Geology 27, 267–270.

Aygül, H., Genç, T., 1999. Marmara bölgesi ve civarının izostasi durumunun gravite, topografya ve batimetri verileri kullanılarak incelenmesi. In: Barka, A., Akyüz, S., Altunel, E., Çakır, Z., (Eds.), Aktif Tektonik II, Türkiye Deprem Vakfı, pp. 121–129.

Barka, A.A., 1992. The North Anatolian Fault Zone. Ann. Tecton. 6, 164–195.

Barka, A.A., Kadinky-Cade, K., 1988. Strike–slip fault geometry in Turkey and its influence on earthquake activity. Tectonics 7, 663–684.

Barka, A.A., Gülen, L., 1989. New constraints on the age and total offset of the North Anatolian Fault Zone: implications for tectonics of the Eastern Mediterranean region. Middle East Tech. Univ. J. Pure Appl. Sci. 21, 39–63.

Barka, A.A., Akyüz, S.H., Cohen, H.A., Watchorn, F., 2000. Tectonic evolution of the Niksar and Tasova-Erbaa pull-apart basins, North Anatolian Fault Zone: their significance for the motion of the Anatolian block. Tectonophysics 322, 243–264.

Ben-Avraham, Z., 1992. Development asymmetric basins along continental transform faults. Tectonophysics 215, 209–220.

Bozkurt, E., 2001. Neotectonics of Turkey – a synthesis. Geodin. Acta 14, 3–30.

Bozkurt, E., Koçyiğit, A., 1996. The Kazova basin: an active negative flower structure on the Almus Fault Zone, a splay fault system of the North Anatolian Fault Zone, Turkey. Tectonophysics 265, 239–254.

Brew, G., Lupa, J., Barazangi, M., Sawaf, T., Al-Imam, A., Zaza, T., 2001. Structure and tectonic development of the Ghab basin and the Dead Sea fault system Syria. Journal of Geological Society, London 158, 665–674.

Chu, D., Gordon, R.G., 1998. Current plate motions across the Red Sea. Geophys. J. Int. 135, 313–328.

Crampin, S., Evans, R., 1986. Neotectonics of the Marmara Sea region of Turkey. J. Geol. Soc. London 143, 343–346.

Dauteuil, O., Huchon, P., Quemeneur, F., Souriot, T., 2000. Propagation of an oblique spreading centre: the western Gulf of Aden. Tectonophysics 332, 423–442.

Ediger, V., Velegrakis, A.F., Evans, G., 2000. Üst Kıta Yamacı Sediman Dalgalanmaları, Kilikya Havzası. In: Uysal, Z. (Ed.), Kuzeydoğu Akdeniz. 1. Deniz Bilimleri Konferansı Bildiri Özetleri Kitapçığı, 30 Mayıs–2 Haziran 2000. Kültür ve Kongre Merkezi ODTÜ, Ankara, 63 pp.

Emre, Ö., Erkal, T., Tchepalyga, A., Kazancı, N., Keçer, M., Ünay, E., 1998. Neogene–Quaternary evolution of the Eastern Marmara Region, Northwest Turkey. Bull. Miner. Res. Explor. Inst. Turk. 120, 119–145.

Ergin, M., Özalaybey, M.T., Aktar, M.T., Tapırdamaz, C., Yörük, A., Biçmen, F., 2000. Aftershock analysis of the August 17, 1999, Izmit, Turkey, earthquake. In: Barka, A., Kozacı, Ö., Akyüz, S., Altunel, E. (Eds.) The 1999 Izmit and Düzce Earthquakes: Preliminary Results. Istanbul Technical University Press, Istanbul, pp. 171–178.

Ergül, E., Gözler, Z., Akçagören, F., Öztürk, Z., 1986. Geology map of Turkey, Bandirma E6 section, Scale 1:10 000. Mineral Research and Exploration of Turkey, Ankara, 10 pp.

Ergün, M., Özel, E., 1995. Structural relationship between the sea of Marmara basin and the North Anatolian Fault. Terra Nova 7, 278–288.

Gazioğlu, C., Gökaşan, E., Algan, O., Yücel, Z.Y., Tok, B., Doğan, E., 2002. Morphologic features of the Marmara Sea from multibeam data. Mar. Geol. 190, S0025-3227(02)00356-0.

Gözler, Z., Cevher, F., Küçükayman, A., 1985. Eskişehir civarının jeolojisi ve sıcak su kaynakları. Bull. Miner. Res. Explor. Turk. 104, 40–54.

Güneysu, A.C., 1999. Bathymetry map of the Izmit Bay. Turk. J. Mar. Sci. 5, 167–170.

Güneysu, C., 1998. Submarine and coastal geomorphology of the Southern Marmara Sea. In: Progress in Marine Geological Studies in Turkey, Tübitak University-MTA, National Marine Geology Programme, Workshop IV, 14–15 May 1998, Istanbul, pp. 166–171.

Gürbüz, C., Aktar, M., Eyidoğan, H., Cisternas, A., Haessler, H., Barka, A., Ergin, M., Türkelli, N., Polat, A., Üçer, S.B., Kuleli, S., Barış, S., Kaypak, B., Bekler, T., Zor, E., Biçmen, F., Yörük, A., 2000. The seismotectonics of the Marmara region (Turkey): results from a microseismic experiment. Tectonophysics 316, 1–17.

Hubert-Ferrari, A., 1998. La Faille Nord-Anatolienne (Cinématique, Morphologie, Localisation, Vitesse et Décalage Total) et Modelisations Utilisant la Contrainte de Coulomb sur

Différentes Echelles de Temps. Ph.D. Thesis. University of Paris VII Denis Diderot, Paris.

Imren, C., Le Pichon, X., Rangin, C., Demirbağ, E., Ecevitoğlu, B., Görür, N., 2001. The North Anatolian fault within the Sea of Marmara: a new interpretation based on multichannel seismic and multi-beam bathymetry data. Earth Planet. Sci. Lett. 186, 143–158.

Kalafat, D., 1995. Anadolu'nun Tektonik Yapılarının deprem Mekanizmaları Açısından Irdelenmesi (in Turkish with English abstract). Unpubl. Ph.D. Thesis. Institute of Marine Sciences and Management, Istanbul University, 217 pp.

Kaymakçı, N., 1991. Neotectonic Evolution of the Inegöl (Bursa) Basin. Unpubl. M.Sc. Thesis. Middle East Technical University, Ankara, 73 pp.

Ketin, I., 1948. Über die tektonisch-mechanischen Folgerungen aus den grossen Anatolischen Erdbeben des letzten Dezenniums. Geol. Rundsch. 36, 77–83.

Ketin, I., 1966. 6 Ekim 1964 Manyas depremi esnasında zeminde meydana gelen tansiyon çatlakları. Türk. Jeol. Kurumu Bül. 10, 1–2.

Ketin, I., 1969. Kuzey Anadolu Fayı Hakkında. Bull. Miner. Res. Explor. Inst. Turk. 76, 1–25.

Koçyiğit, A., 1988. Tectonic setting of the Geyve basin: age and total displacement of Geyve fault zone. METU Pure Appl. Sci. 21, 81–104.

Koçyiğit, A., 1989. Suşehri basin: an active fault-wedge basin on the North Anatolian Fault Zone, Turkey. Tectonophysics 167, 13–29.

Koçyiğit, A., 1991. Neotectonic structures and related landforms expressing the contractional and extensional strains along the North Anatolian Fault at the northwestern margin of the Erzincan Basin, NE Turkey. Bull. Tech. Univ. Istanbul 44, 455–473.

Le Pichon, X., Taymaz, T., Şengör, A.M.C., 1999. The Marmara Fault and the future Istanbul Earthquake. Proc. ITU-IAHS International Conference on the Kocaeli Earthquake, Istanbul, pp. 41–54.

Marathon Petroleum, 1976. Marmara-1 well. Final Report, 26 pp.

McKenzie, D., 1972. Active tectonics of the Mediterranean region. Geophys. J. R. Astron. Soc. 30, 109–185.

Okay, A., Demirbağ, E., Kurt, H., Okay, N., Kuşçu, I., 1999. An active, deep marine strike–slip basin along the North Anatolian fault in Turkey. Tectonics 18, 129–147.

Okay, A., Kaşlılar-Özcan, A., Imren, C., Boztepe-Güney, A., Demirbağ, E., Kuşçu, I., 2000. Active faults and evolving strike–slip basins in the Marmara Sea, northwest Turkey: a multichannel seismic reflection study. Tectonophysics 321, 189–218.

Parke, J.R., Minshull, T.A., Anderson, G., White, R.S., McKenzie, D., Kuşçu, I., Bull, J.M., Görür, N., Şengör, C., 1999. Active faults in the Sea of Marmara, Western Turkey, imaged by seismic reflection profiles. Terra Nova 11, 223–227.

Perinçek, D., 1991. Possible strand of the North Anatolian Fault in the Thrace Basin, Turkey: an interpretation. Am. Assoc. Pet. Geol. Bull. 75, 241–257.

Sakınç, M., Yaltırak, C., Oktay, F.Y., 1999. Palaeogeographical evolution of the Thrace Neogene Basin and the Tethian-Paratethian relations at northwest Turkey (Thrace). Palaeogeogr. Palaeoclimatol. Palaeoecol. 153, 17–40.

Şaroğlu, F., 1988. The age and offset on the North Anatolian Fault. Middle East Tech. Univ. J. Pure Appl. Sci. 21, 65–79.

Şengör, A.M.C., 1979. The North Anatolian Transform Fault: its age, offset and tectonic significance. J. Geol. Soc. London 136, 269–282.

Şengör, A.M.C., 1980. Türkiye'nin Neotektoniğinin Esasları 'Principles of the Neotectonism of Turkey'. Türkiye Jeoloji Kurumu, Ankara, 40 pp.

Şengör, A.M.C., Görür, N., Şaroğlu, F., 1985. Strike–slip faulting and related basin formation in zones of tectonic escape: Turkey as a case study. In: Biddle, K.T., Christie-Blick, N. (Eds.), Strike–slip Faulting and Basin Formation. Soc. Econ. Paleontol. Mineral. Spec. Publ. 37, 227–264.

Sylvester, A.G., 1988. Strike–slip faults. Geol. Soc. Am. Bull. 100, 1666–1703.

Siyako, M., Bürkan, K.A., Okay, A.I., 1989. Biga ve Gelibolu yarımadalarının Tersiyer jeolojisi ve hidrokarbon olanakları. Bull. Turk. Assoc. Pet. Geol. 1, 183–199.

Siyako, M., Tanış, T., Şaroğlu, F., 2000. Marmara Denizi aktif fay geometrisi. TÜBITAK Bilim Tek. Derg. 388, 66–71.

Smith, A.D., Taymaz, T., Oktay, F.Y., Yüce, H., Alpar, B., Başaran, H., Jackson, J.A., Kara, S., Şimşek, M., 1995. High-resolution seismic profiling in the Sea of Marmara (northwest Turkey): late Quaternary sedimentation and sea-level changes. Geol. Soc. Am. Bull. 107, 923–936.

Straub, C., Kahle, H.G., Schindler, C., 1997. GPS and geologic estimates of the tectonic activity in the Marmara Sea region, NW Anatolia. J. Geophys. Res. Solid Earth B12, 27587–27601.

Tapırdamaz, C., Yaltırak, C., 1997. Trakya'da Senozoyik volkaniklerinin paleomanyetik özellikleri ve bölgenin tektonik evrimi. Bull. Min. Res. Explor. Turk. 119, 27–42.

Taymaz, T., 1990. Earthquake Source Parameters in the Eastern Mediterranean Region. Ph.D. Thesis. Cambridge University, Cambridge, 244 pp.

Taymaz, T., 1999. Seismotectonics of the Marmara region: Source characteristics of 1999 Gölcük-Sapanca-Düzce earthquakes. Proc. ITU-IAHS, International Conference on the Kocaeli Earthquake 17 August 1999, Istanbul, pp. 55–78.

Taymaz, T., 2000. Seismotectonics of the Marmara region: source characteristics of 1999 Gölcük-Sapanca-Düzce earthquakes. In: Barka, A.A., Kozacı, Ö., Akyüz, S.H., Altunel, E. (Eds), 1999 Izmit-Düzce Earthquakes: Preliminary Results. Istanbul Technical University Publ., Istanbul, pp. 79–97.

Taymaz, T., Jackson, J., McKenzie, D.P., 1991. Active tectonics of the North and Central Aegean Sea. Geophys. J. Inter. 106, 433–490.

Taymaz, T., Kasahara, J., Hirn, A., Sato, T., 2001. Investigations of microearthquake activitiy within the Sea of Marmara and surrounding regions by using ocean bottom seismometers (OBS) and land seismographs: Initial results. In: Taymaz, T. (Ed.), Symposia on Seismotectonics of the

North-Western Anatolia-Aegean and Recent Turkish Earthquakes. Scientific Activities 2001, May 8, 2001. Faculty of Mines, Istanbul Technical University, Istanbul, pp. 42–51.

Toprak, V., 1988. Neotectonic characteristics of the North Anatolian fault zone between Koyulhisar and Suşehri (NE Turkey). Middle East Tech. Univ. J. Pure Appl. Sci. 21, 155–168.

Tüysüz, O., Barka, A.A., Yiğitbaş, E., 1998. Geology of the Saros Graben: its implications on the evolution of the North Anatolian Fault in the Ganos-Saros region, NW Turkey. Tectonophysics 293, 105–126.

Ünay, E., Emre, Ö., Erkal, T., Keçer, M., 2001. The rodent fauna from the Adapazarı pull-apart basin (NW Anatolia): its bearings on the age of the North Anatolian Fault. Geodin. Acta 14, 169–175.

Wong, H.K., Ludmann, T., Uluğ, A., Görür, N., 1995. The Sea of Marmara, a plate boundary sea in escape tectonic regime. Tectonophysics 244, 231–250.

Wright, T., Parsons, B., Fielding, E., 2001. The 1999 Turkish earthquakes: source paramaters from InSAR and observations of triggered slip. In: Taymaz, T. (Ed.), Symposia on Seismotectonics of the North-Western Anatolia-Aegean and Recent Turkish Earthquakes. Scientific Activities 2001, May 8, 2001. Faculty of Mines, Istanbul Technical University, Istanbul, pp. 54–71.

Yaltırak, C., 1996. Tectonic history of the Ganos Fault system (in Turkish with English abstract). Bull. Turk. Assoc. Pet. Geol. 8, 137–156.

Yaltırak, C., 2000a. Kuzey Anadolu fayının Marmara kolları ve bölgenin tektonik yapısı (in Turkish). Guney Marmara Depremleri ve Jeofizik Toplantısı, TMMOB Jeofizik Mühendisleri Odasi, 22 September 2000, Bursa, pp. 44–48.

Yaltırak, C., 2000b. Problem of Marmara (in Turkish with English abstract). In: Uysal, Z., Salihoğlu, I. (Eds.), 1st National Marine Science Conferences, May 30–June 2, 2000. Middle East Technical University, Ankara, pp. 202–207.

Yaltırak, C., Alpar, B., 2002a. Kinematics and evolution of the Northern Branch of the North Anatolian Fault (Ganos Fault) between the Sea of Marmara and the Gulf of Saros. Mar. Geol. 190, S0025-3227(02)00354-7.

Yaltırak, C., Alpar, B., 2002b. Evolution of the middle strand of North Anatolian Fault and shallow seismic investigation of the Southeastern Marmara Sea (Gemlik Bay). Mar. Geol., this volume.

Yaltırak, C., Alpar, B., Yüce, H., 1998. Tectonic elements controlling the evolution of the Gulf of Saros (Northeastern Aegean Sea). Tectonophysics 300, 227–248.

Yaltırak, C., Sakınç, M., Oktay, F.Y., 2000a. Westward propagation of the North Anatolian fault into the northern Aegean: timing and kinematics, Comment. Geology 28, 187–188.

Yaltırak, C., Alpar, B., Sakınç, M., Yüce, H., 2000. Origin of the Strait of Çanakkale (Dardanelles): regional tectonics and the Mediterranean – Marmara incursion. Mar. Geol. 164, 139–156, with erratum 167, 189–190.

Yılmaz, B., 1996. Marmara Denizinde Büyükçekmece (Istanbul) Marmara Ereğlisi (Tekirdağ) kıyı kesimini jeolojisi (in Turkish with English summary). Unpublished M.Sc. Thesis. Istanbul Technical University, 61 pp.

Yılmaz, Y., Polat, A., 1998. Geology and Evolution of the Thrace volcanism, Turkey. Acta Vulcanol. 10, 293–303.